71-4039

HOGE, Albert Russell, 1943-
HYDROGENATION OF ALPHA-METHYLSTYRENE IN A TRICKLE-BED REACTOR EMPLOYING A NON-POROUS CATALYST.

University of Maryland, Ph.D., 1970
Engineering, chemical

University Microfilms, Inc., Ann Arbor, Michigan

Reproduced with permission of the copyright owner. Further reproduction prohibited without permission.

HYDROGENATION OF ALPHA-METHYLSTYRENE IN A TRICKLE-BED REACTOR EMPLOYING A NON-POROUS CATALYST

by

Albert Russell Hoge

Dissertation submitted to the Faculty of the Graduate School
of the University of Maryland in partial fulfillment
of the requirements for the degree of
Doctor of Philosophy
1970

Reproduced with permission of the copyright owner. Further reproduction prohibited without permission.

APPROVAL SHEET

Title of Thesis: HYDROGENATION OF ALPHA-METHYLSTYRENE IN A TRICKLE-BED REACTOR EMPLOYING A NON-POROUS CATALYST

Name of Candidate: Albert Russell Hoge
Doctor of Philosophy, 1970

Thesis and Abstract Approved: Theodore G. Smith

Dr. Theodore G. Smith
Associate Professor
Chemical Engineering

Date Approved: April 4, 1970

Reproduced with permission of the copyright owner. Further reproduction prohibited without permission.

ABSTRACT

Title of Thesis: HYDROGENATION OF ALPHA-METHYLSTYRENE IN A TRICKLE-BED REACTOR EMPLOYING A NON-POROUS CATALYST

Albert Russell Hoge, Doctor of Philosophy, 1970

Thesis directed by: Associate Professor Theodore G. Smith

The study reported here is an experimental investigation of the catalytic hydrogenation of alpha-methylstyrene in a trickle-bed reactor and an analysis of the results in terms of a kinetic model. A major objective of the study was to demonstrate that isothermal intrinsic reaction rates can be measured in a trickle-bed reactor. In all previously reported trickle-bed studies, porous catalysts have been used and thus reported reaction rates have included pore diffusion effects. In addition, previous work has shown that when highly exothermic reactions are studied in a differential bed reactor, significant temperature gradients can exist especially when active catalyst is concentrated in a small reactor volume. In the present investigation an attempt was made to eliminate pore diffusion resistances by employing a catalyst consisting of palladium deposited on the surface of irregular granules of a non-porous mineral,

Reproduced with permission of the copyright owner. Further reproduction prohibited without permission.

dolomite. Near-isothermal conditions were maintained in the reactor by diluting the active catalyst with inert granules of dolomite which served as a heat sink and liquid distributor.

A bed height of 4.5 inches was used in a three inch I.D. Pyrex reactor. The average granule diameter was 1.61 mm. and the catalyst dilution ratio was 100 grams of catalyst to 600 grams of inert dolomite. Reaction rate data were obtained at 32, 40, and 50° C and at one atmosphere hydrogen pressure. The liquid feed stream consisted entirely of alpha-methylstyrene which flowed at rates between 100 and 225 cc./min. The hydrogen flow rate ranged from 1.0 to 2.5 liters/min. Effluent liquid phase composition was determined with a gas chromatograph.

It was found that the catalyst activity decreased with time due to poisoning of the catalyst surface by copper which had dissolved in the alpha-methylstyrene. The intrinsic reaction rate data was described, within an accuracy of about 10%, by a kinetic model which assumes plug flow in the liquid phase, the activity of the catalyst decreases exponentially with time, and the surface reaction rate is first order in hydrogen pressure. The calculated activation energy for reaction, 7,280 cal./gm. mole, agrees

Reproduced with permission of the copyright owner. Further reproduction prohibited without permission.

well with previously reported values. Kinetic rate constants also show good agreement with published values obtained on other types of palladium catalysts.

Reproduced with permission of the copyright owner. Further reproduction prohibited without permission.

ACKNOWLEDGMENTS

The author is indebted to three companies whose contributions of materials made this investigation possible. Houdry Process and Chemical Company donated the palladium catalyst and the inert dolomite employed. Mr. Hans Hansen of Engelhard Minerals and Chemicals Corp. arranged for the author to have samples of palladium-on-alumina catalysts. Large quantities of alpha-methylstyrene and cumene were donated by Dow Chemical Company through the efforts of Mr. James E. Townsend, Jr.

To the author's advisor, Dr. Theodore G. Smith, goes a very special expression of appreciation for his guidance and encouragement. Helpful suggestions were made by Drs. A. Gomezplata and T. W. Cadman.

For their invaluable assistance in purchasing and constructing the equipment, the author thanks Messrs. John Smith and Aylor Hodnett. Also acknowledged is Mr. Kenneth Rayburn of the Chemistry Department at the University of Maryland who performed the optical emission spectral analyses. Informal discussions with fellow graduate students led to some helpful ideas. In particular, the comments of Mr. Ira Felsen and Dr. Hussein Taha were appreciated.

Reproduced with permission of the copyright owner. Further reproduction prohibited without permission.

The author thanks the Chemical Engineering Department for financial assistance in the form of a teaching assistantship and an NDEA Fellowship.

Computer time was provided by the Computer Science Center at the University of Maryland under NASA Grant NSG - 398.

For their fine work in typing this manuscript and in preparing the figures, the author extends his thanks to Mrs. Suzanne Collins and Mr. James Dashiell, respectively.

The author is grateful to Professor C. N. Satterfield of the Massachusetts Institute of Technology for permission to reproduce the physical property data presented in the figures in Appendix C.

By far the greatest contribution was made by the author's wife, Lynne, and daughter, Nancy. Their patience, encouragement, and devotion were unfailing during times of trial. Lynne's assistance in preparing the manuscript was invaluable.

The author and his family are particularly indebted to his parents for their moral and financial support throughout the period of his graduate studies.

Reproduced with permission of the copyright owner. Further reproduction prohibited without permission.

TABLE OF CONTENTS

Chapter		Page
ACKNOWLEDGMENTS		ii
INTRODUCTION		1
I.	LITERATURE SURVEY	4
	A. Kinetics in Trickle-Bed Reactors	4
	B. Two Phase Flow Data	8
	C. Axial and Radial Dispersion Studies	10
	D. Mass Transfer in Packed Bed Reactors	17
	E. Diluted Catalyst Beds	19
II.	EQUIPMENT AND OPERATING PROCEDURE	21
	A. Equipment	21
	B. Operating Procedure	27
III.	RESULTS	33
	A. Effect of Poisoning	36
	B. Effect of Gas Flow Rate	46
	C. Effect of Liquid Flow Rate	46
	D. Effect of Temperature	51
	E. Effect of Catalyst Weight	51
IV.	DISCUSSION OF RESULTS	57
	A. Development of the Model	57
	1. Fluid Hydrodynamics	57
	2. Individual Pellet Kinetics	60

Reproduced with permission of the copyright owner. Further reproduction prohibited without permission.

Chapter Page

Physical Steps 60

Chemical Kinetic Steps 65

B. Interpretation of Results 77

V. CONCLUSIONS AND RECOMMENDATIONS 84

APPENDIX A. CHROMATOGRAPHIC ANALYSIS 87

APPENDIX B. OPERATING CONDITIONS AND CATALYST DATA 90

APPENDIX C. PHYSICAL PROPERTIES OF THE FLUIDS . . . 94

NOMENCLATURE 100

LITERATURE CITED 104

Reproduced with permission of the copyright owner. Further reproduction prohibited without permission.

LIST OF TABLES

Table		Page
III-1.	Reaction Rate Data at 32° C	41
III-2.	Reaction Rate Data at 40° C	42
III-3.	Reaction Rate Data at 50° C	43
B-1.	Data on Catalyst and Reactor Bed	91
B-2.	Summary of Run Conditions	92

Reproduced with permission of the copyright owner. Further reproduction prohibited without permission.

LIST OF FIGURES

Figure		Page
II-1.	Flow Diagram of Apparatus	22
II-2.	Schematic Diagram of Trickle-Bed Reactor . .	23
III-1.	Reaction Rate as a Function of Process Time at 32° C	37
III-2.	Reaction Rate as a Function of Process Time at 40° C	38
III-3.	Reaction Rate as a Function of Process Time at 50° C	39
III-4.	Reaction Rate as a Function of Process Time for Run 40 at 32° C	45
III-5.	Effect of Gas Flow Rate on Intrinsic Rate Constant for L = 100 cc./min. at 50° C	47
III-6.	Effect of Gas Flow Rate on Intrinsic Rate Constant for All Liquid Flow Rates	48
III-7.	Effect of Liquid Flow Rate on Intrinsic Rate Constant for G = 1.0 liters/min. at 40° C	49
III-8.	Effect of Liquid Flow Rate on Intrinsic Rate Constant for All Gas Flow Rates	50
III-9.	Arrhenius Plot of Intrinsic Rate Constant versus the Reciprocal of Absolute Temperature	52
III-10.	Weight Percent Cumene in the Reactor Effluent as a Function of Time for Run 10	54

Reproduced with permission of the copyright owner. Further reproduction prohibited without permission.

Figure		Page
III-11.	Reaction Rate as a Function of Active Catalyst Weight for Five Runs at 32° C	55
C-1.	Densities of Alpha-methylstyrene and Cumene as Functions of Temperature	95
C-2.	Vapor Pressure of Alpha-methylstyrene as a Function of Temperature	96
C-3.	Viscosity of Alpha-methylstyrene as a Function of Temperature	97
C-4.	Diffusivity of Hydrogen in Alpha-methylstyrene as a Function of Temperature	98
C-5.	Solubility of Hydrogen in Alpha-methylstyrene as a Function of Temperature at One Atmosphere Pressure	99

Reproduced with permission of the copyright owner. Further reproduction prohibited without permission.

INTRODUCTION

A trickle-column reactor, in which the gas and liquid phases pass downward cocurrently over a fixed bed of catalyst granules, has been commercially employed by the chemical industry for about seventeen years. In its first application as a hydrodesulfurizer, the three phase trickle-bed reactor was found to be 15 to 20% cheaper to operate than the equivalent vapor phase reactor. Since that time, the trickle-bed reactor has demonstrated its utility in many reaction engineering applications.

A trickle-bed reactor has several advantages over stirred tanks in carrying out catalyzed gas-liquid reactions. If properly operated the three phases are brought into intimate contact without the need for vigorous mechanical agitation. The thickness of the liquid film covering the catalyst is small, whereas the area of the liquid film is very large by comparison with that in a stirred reactor. This insures rapid diffusion of gas to the catalyst surface and minimizes the chances of having a reaction rate limited by diffusion. The reaction product is formed continuously and no catalyst filtration step is necessary. With the correct choice of catalyst, these reactors can be operated

Reproduced with permission of the copyright owner. Further reproduction prohibited without permission.

at relatively low temperatures and pressures and thus undesirable side reactions can often be minimized.

Since many oxidation and hydrogenation reactions are highly exothermic, one difficulty often encountered in trickle-bed reactors is inadequate temperature control. Even the use of thin differential beds of catalyst may not provide adequate temperature regulation and thus they have not proven entirely satisfactory for intrinsic reaction studies. Additionally, in all of the laboratory studies reported to date, porous catalysts have been employed to measure reaction rates. As a result, no kinetic investigations have been entirely free of diffusion limitations (either external or pore-type). These diffusional effects are often difficult to account for and, therefore, the intrinsic reaction rate data is of questionable accuracy.

The present investigation was undertaken to demonstrate that true intrinsic reaction rates can be measured in a trickle-bed reactor. As used in this thesis the term intrinsic reaction rate is defined as the surface reaction rate measured in a system in which all mass transfer resistances are insignificantly small. To combat the temperature problem, the active catalyst was mixed with a large volume of inert granules which served as a heat sink and liquid distributor. Pore diffusion effects were eliminated

Reproduced with permission of the copyright owner. Further reproduction prohibited without permission.

by the use of a non-porous catalyst support, dolomite. By properly choosing the gas and liquid flow rates, external diffusion limitations did not exist.

In the kinetic study reported here, alpha-methylstyrene was hydrogenated to cumene over a catalyst consisting of 0.3 weight percent palladium deposited on the surface of irregular 10-16 mesh dolomite granules. One hundred grams of catalyst were diluted with six hundred grams of inert dolomite of the same size and packed to a depth of 4.5 inches in a 3 inch I.D. Pyrex reactor. Liquid flow rates varied between 100 and 225 cc./minute and the hydrogen rates ranged from 1.0 to 2.5 liters/minute. Reaction rates were measured at temperatures of 32, 40, and 50^{o} C.

Reproduced with permission of the copyright owner. Further reproduction prohibited without permission.

CHAPTER I

LITERATURE SURVEY

A review of the literature pertaining to the present research falls naturally into four primary areas; kinetics in trickle-bed reactors, two phase flow data, axial and radial dispersion studies, and mass transfer in packed bed reactors. Additional literature of particular interest to this investigation is presented in a fifth section.

A. Kinetics in Trickle-Bed Reactors

Trickle-bed reactors were introduced commercially in 1953 (30) as an economical means of removing sulfur from petroleum fractions. The trickle technique, in which liquid feed flows downward as a film over catalyst pellets and contacts hydrogen gas also in downflow, was superior to the equivalent vapor phase operation in that capital investment and operating costs were reduced by 15 to 20%. It was found that sulfur removal (as H_2S) of 85 to 90% could be obtained and that the catalyst had long life without the need for regeneration. An interesting discussion of the chronological development of Shell's hydrodesulfurization process is given by van Deemter (66).

Reproduced with permission of the copyright owner. Further reproduction prohibited without permission.

Since 1953 several industrial applications of gas-liquid packed bed reactors have been reported in the literature (15, 26, 65). Generally these processes involve the hydrocracking of petroleum distillates and, therefore, are extensively employed in modern refinery operations.

Klassen and Kirk (35) studied the kinetics of the liquid phase oxidation of ethanol to acetic acid in a countercurrent trickle-bed reactor. The proposed model of the process was based on a concentric series of liquid and gas films around a catalyst pellet. The equation describing the observed rates over palladium-on-alumina catalyst included a kinetic term and a mass transfer term for the diffusion of oxygen. The reaction rate was controlled by mass transfer resistances in both the gas and liquid films and by surface reaction kinetics. Intrinsic reaction rate was determined by varying reactant concentrations, while mass transfer resistances were evaluated by varying gas and liquid flow rates.

Babcock, Mejdell, and Hougen (6) also used a countercurrent trickle-bed reactor to conduct a kinetic study of the hydrogenation of alpha-methylstyrene to cumene. The catalysts employed were palladium, platinum, rhodium, ruthenium, and nickel supported on alumina pellets. Quantitative results for only the platinum and palladium catalysts

Reproduced with permission of the copyright owner. Further reproduction prohibited without permission.

were presented. Rhodium and ruthenium catalysts were not active enough to reliably measure reaction rates and nickel polymerized the alpha-methylstyrene. The rate-controlling step on platinum and palladium catalysts was correlated by adsorption isotherm equations of the Langmuir-Hinshelwood type. Operating temperatures ranged from 24.3° C to 57.2° C and pressures from 1.93 atmospheres to 12 atmospheres. On palladium catalysts and above three atmospheres pressure, the rate-controlling step was the surface reaction between dissociated hydrogen and alpha-methylstyrene, each adsorbed on different types of active sites. Below three atmospheres the only data taken exhibited a maximum in reaction rate at 60 mole percent alpha-methylstyrene. This behavior was explained by assuming the rate was controlled by the competition of hydrogen and alpha-methylstyrene for the same active catalyst sites. The authors attributed this change in the rate-controlling step with increase in pressure to a transition of the palladium-hydrogen system from the α to the β phase. Platinum catalysts exhibited extreme variation in activity and rate equations were expressed in terms of a standard activity factor. It has recently been suggested (47) that, due to a miscalculation of the catalyst effectiveness factor, the measurements of Babcock et al. were strongly influenced by pore diffusion and their analysis is therefore erroneous.

Reproduced with permission of the copyright owner. Further reproduction prohibited without permission.

Acres (2) presents reaction rate data on the hydrogenation of several classes of organic compounds in a trickle-bed reactor. He emphasizes the point that many reactions can be carried out at less severe operating conditions in a trickle-bed than in other types of reactors. He proposes that a partial solution to the problem of maldistribution of the liquid phase in a trickle-bed is to use irregularly shaped granular pellets as the packing and active catalyst. This shape of pellet should be an improvement over cylindrical pellets, which tend to stack and cause severe channeling, and over spherical packings which can promote excessive flow along the reactor wall.

In a British patent, Acres and Budd (4) employed a palladium catalyst in a trickle-bed reactor to selectively hydrogenate crotonaldehyde. The authors claim a 70 percent improvement over the equivalent fixed bed gas phase hydrogenation on a copper catalyst.

One of the most recent investigations of trickle-bed kinetics is the work of Pelossof (47, 52). The primary objective of the study was to determine the role played in trickle-bed performance by the resistance of the liquid film to mass transfer of the reacting gas. Alpha-methylstyrene was hydrogenated to cumene at one atmosphere total pressure in the temperature range 20° C to 50° C. In order to

Reproduced with permission of the copyright owner. Further reproduction prohibited without permission.

circumvent the potential maldistribution problems of a packed bed, Pelossof's reactor consisted of a single, suspended vertical column of spherical, porous palladium-on-alumina catalyst pellets 0.825 cm. in diameter. Overall kinetics, including surface reaction kinetics, pore diffusion resistance, and liquid film mass transfer limitations, were measured in the suspended sphere reactor. The individual contributions of pore diffusion and intrinsic surface kinetics were determined separately in a special stirred tank reactor. From a mass balance on hydrogen (the limiting reactant) in the liquid film surrounding a single pellet, two mathematical models were developed to predict the concentration profile across the film. The mass transfer coefficients predicted by these models were compared with the stagnant film and penetration theory predictions. The correct agreement was obtained between the corresponding models.

B. Two Phase Flow Data

Because of the industrial importance of fluid flow in packed beds, there is considerable literature now available concerning the characterization of these beds. Information on both two phase flow (cocurrent and countercurrent) and single phase flow in packed beds is appearing at an ever increasing rate in the literature. Typical types of data

Reproduced with permission of the copyright owner. Further reproduction prohibited without permission.

which are presented are pressure drop, liquid holdup, and liquid loading behavior.

A majority of the articles concerning cocurrent two phase flow in packed beds have appeared in the past decade. The most frequently studied systems employed air and water as fluids and Raschig rings or Berl saddles from 1/4" to 2" in diameter as packing materials.

Larkins et al. (38) measured pressure drop and liquid holdup in a variety of packings and with gas-liquid systems having a wide range of fluid properties. Single phase friction loss data for each phase flowing alone in the bed must be available to utilize the two phase correlation which is presented. Reiss (49) found Larkins' correlation quite adequate, whereas Charpentier et al. (13) suggested a slight modification to it. Another pressure drop correlation based on the existence of single phase pressure drop data has also been presented (61).

Weekman and Myers (72) extended a well-known correlation of two phase flow in pipes to include two phase flow in packed beds. The packed bed correlations for pressure drop and liquid holdup agreed well with the data. Semi-empirical pressure drop correlations by two other authors (64, 74) are available but it is probably dangerous to extrapolate them to other systems.

Reproduced with permission of the copyright owner. Further reproduction prohibited without permission.

Ross (50) compared the performances of three different sizes of trickle-bed reactors. He measured residence time distributions, liquid holdups, and sulfur removal rates in a hydrodesulfurization reaction. A comparison of conversion data indicated that reduced reaction efficiency in the commercial unit was due to poor distribution of liquid over the commercial catalyst bed. Therefore, improvements in commercial reactor design are necessary.

Gas absorption, pressure drop, liquid holdup, and loading behavior in a packed column were investigated by Coughlin (14) using geometrically identical packings which were made from three different packing materials. Both pressure drop and operating holdup were independent of the type of packing material.

C. Axial and Radial Dispersion Studies

The axial and radial distribution of fluids in motion in a packed bed has been a topic of discussion among researchers for many years. The original analyses of the flow distributions and the extent of mixing in packed beds were concerned with single phase flow only. However, in recent years with the development of packed absorption columns, trickle-bed reactors, and so on, extensions of the analyses to two phase flow has been necessary. For a thorough

Reproduced with permission of the copyright owner. Further reproduction prohibited without permission.

discussion of the mixing characteristics of many types of single phase and two phase contactors the reader is referred to a review by Bischoff (7). Aside from the plug flow model in which the flowing phases are assumed to have flat velocity profiles with no radial variations, two types of mathematical models have most frequently been used to describe the degree of axial mixing in a packed bed. These are the axial dispersion model and the stirred-tanks-in-series or mixing-cell model.

The axial dispersion model assumes that deviations from ideal flow are caused by a large number of small random movements by fluid molecules. This model has been used by several investigators to describe both single phase (12, 19, 48) and two phase flow (29, 51) in packed beds. Bischoff (8), in a discussion of the applicability of the axial dispersion model to chemical reactors, concludes that the model should be most accurate for describing slow reactions in long reactors. With regard to gas flow through packed beds, Carberry and Bretton (12) and Edwards and Richardson (19) both conclude that at Reynolds numbers less than one, the axial dispersion is controlled by molecular diffusion and the dispersion coefficient is approximately equal to the molecular diffusivity. Above a Reynolds number of about 10, turbulent or eddy diffusion predominates.

Reproduced with permission of the copyright owner. Further reproduction prohibited without permission.

Carberry and Bretton (12) also measured the dispersion coefficient for water in the range of Reynolds numbers from 0.5 to 400. A linear relationship existed between the dispersion coefficient and the Reynolds number in the 0.5 to 100 range. At a Reynolds number of unity, the dispersion coefficient had a value of about 10^{-2} $cm.^2/sec.$, corresponding to very small dispersion. Raines and Corrigan (48) applied the axial dispersion model to a liquid phase packed bed reactor. At Reynolds numbers near unity, the model predictions of the conversions for both first order and second order reactions agreed well with the experimental data. At low Reynolds numbers the extent of dispersion was small and was approximated well by a plug flow model. Below a bed length to packing diameter ratio of about twenty to one, care should be exercised in choosing the proper boundary conditions for the dispersion equation. Hofmann (29) was one of the first investigators to present axial dispersion data for two phase flow systems. His results were graphically presented as axial Peclet numbers as a function of Reynolds and Schmidt numbers with gas flow rate as a parameter on the graphs. More recently, Sater and Levenspiel (51) studied the extent of axial dispersion in both the gas and liquid phases in a bed packed with 1/2 inch Raschig rings or Berl saddles. The results indicate that large

Reproduced with permission of the copyright owner. Further reproduction prohibited without permission.

deviations from plug flow exist in both fluid phases. However, this non-ideality would be expected at the large Reynolds numbers employed ($0 < N_{Re_L} < 300$ and $50 < N_{Re_G} < 180$).

The stirred-tanks-in-series or mixing-cell model assumes that a fixed bed consists of a series of perfectly mixed regions in the interstices of a bed of granules which are connected by flow paths. This type of model is popular primarily because it is computationally easier to use than the dispersion model. Some of the computational aspects of this model, as applied to both non-reactive and chemically reactive systems, have been considered by Deans and Lapidus (16, 17). Taha (63) has recently applied a one-dimensional mixing-cell model to a gas-solid reactive system. While the model did correlate the experimental data well, it was found that a simple plug flow model described the hydrodynamics almost equally as well and with far more computational ease. The "best" stirred tank model had seven stages and apparent plug flow behavior was achieved with only twelve stirred tanks. Jeffreson (33) recently extended the model to allow for intraparticle diffusion effects. The results show good agreement with the axial dispersion model over a wide range of parameters. The reader should refer to Bischoff (7) for a more complete discussion of the mixing-cell model.

Other models which account for axial mixing and

Reproduced with permission of the copyright owner. Further reproduction prohibited without permission.

dispersion in fixed beds have recently appeared in the literature (23, 24, 27, 31, 69). Levenspiel and Bischoff (39) present a review and discussion of some of these models. In general, these new models consist of combinations of existing simple models and concepts. For example, the packed bed could be described by a dispersion model with bypassing or dead zones, or by a series of stirred tanks with recycle between certain stages, and so forth. Three papers (27, 31, 69) propose a model for the liquid phase behavior which assumes exchange of mass between free-flowing regions and stagnant zones. Three parameters, the fraction plug flow, the exchange coefficient, and the mean residence time characterize such a model. Hoogendoorn and Lips (31) and van Swaaij and coworkers (69) studied only air-water flow over Raschig rings and found the model to be applicable at liquid Reynolds numbers above 10. Gas flow rates (up to the loading point) had little or no effect on the degree of dispersion. In one paper (69), the degree of axial dispersion of the liquid phase was well correlated with the ratio of dynamic holdup to static holdup. Hochman and Effron (27) studied cocurrent trickle flow of methanol and nitrogen over 3/16" glass beads. Radial velocity variations were small. Gas phase dispersion increased with increasing liquid Reynolds number, but at liquid Reynolds numbers near unity

Reproduced with permission of the copyright owner. Further reproduction prohibited without permission.

very little gas dispersion existed. This effect was attributed to liquid bridging between the packings. That is, the flowing gas phase essentially sees agglomerates of particles covered by bridging liquid films. Significant liquid dispersion was observed, especially at low Reynolds numbers. However, this result would certainly be expected in a long bed (8 feet) due to problems in packing the bed uniformly.

Two studies by Glaser and his coworkers (23, 24) discuss the problems encountered in using porous packings that cannot be accounted for by axial dispersion or similar models. In flow over porous packings the simple axial dispersion model does not consider potential capacitance effects in the bed such as fluid diffusion within the pores which produces a long tail on the residence time curves. Diffusion effects, particularly pore diffusion, are significant at low liquid flow rates. In conclusion it should be noted that, despite the apparent successes of some of these so-called "mixed models" in correlating the data from specific experiments, care should be exercised in employing them. Extrapolations of such models to complicated systems would be difficult because of the numerous parameters which are sometimes involved and because of the danger of "curve-fitting" instead of truly modeling a physical system.

Reproduced with permission of the copyright owner. Further reproduction prohibited without permission.

Radial distribution of fluids in a packed bed has been the subject of much discussion. Hoftyzer (28), in measurements with one inch Raschig rings, found that irregular surface wetting was a problem in dumped packings but that the distribution of the liquid over the cross section of the column was very even. Among others who have done work on describing radial liquid distributions are Dutkai and Ruckenstein (18) whose particular interest was in characterizing the extent of flow along the wall. A disproportionate amount of liquid will frequently flow along the wall where the void fraction is greatest. The extent of wall flow is largely dependent on the ratio of the column diameter to the packing size. The critical value of this ratio above which radial maldistribution of liquid is insignificant is difficult to determine. For many years an acceptable value was taken to be 10/1. However, the data of Schiesser and Lapidus (54) indicate heavy wall flows even at a ratio of 16/1. Improvements in the profile were evident in increasing the ratio from 8/1 to 16/1. One can conclude that, in order to eliminate a disproportionate wall flow and to produce an even radial liquid distribution, one should operate at a tube diameter to pellet diameter ratio of at least 25/1 or 30/1.

Of particular importance to the present study were the

Reproduced with permission of the copyright owner. Further reproduction prohibited without permission.

results of Lapidus (37) and Schiesser and Lapidus (54). Residence time studies were reported for cocurrent downflow of air-water and air-hydrocarbon in a two inch diameter packed column. These data, as well as other data obtained in columns ranging in diameter from 3/4 inch to 6 feet, indicated that the liquid phase approached plug flow behavior. The liquid phase was particularly well behaved (near plug flow) when non-porous packings were used. When porous packings were employed, internal diffusion effects changed the shape of the residence time curves. Murphree et al. (43) presented some interesting results for a two phase, cocurrent downflow, fixed bed reactor. Residence time distribution studies were used to determine the performance of a hydrodesulfurization reactor. With a first order or pseudo first order reaction the residence time distribution can be used to completely characterize the reactor performance. The results indicated that commercial sized desulfurizers can deviate significantly from plug flow behavior. However, the pilot plant reactor showed a close approach to plug flow.

D. Mass Transfer in Packed Bed Reactors

Typical examples of gas-liquid mass transfer operations employing packed beds are absorption or desorption columns and humidification or dehumidification columns. Dissolution operations also exist in which solid-liquid mass transfer

Reproduced with permission of the copyright owner. Further reproduction prohibited without permission.

applies. Since trickle-beds do involve three phase contacting, an analysis of the mass transfer literature should be helpful.

For solids dissolving into liquids, two forms of correlations are found (68, 76, 77). van Krevelen and Krekels (68) related the Sherwood number to the one-half power of Reynolds number and to the one-third power of the Schmidt number for film-like flow at Reynolds numbers less than 20. Other authors (76, 77) preferred to use the "J" notation, where $J = \left(\frac{k_L}{U_L}\right) (N_{Sc})^m = S(N_{Re})^P$. The values of S and P depend upon the magnitude of the Reynolds number. The constant m equals two-thirds according to (77) while Williamson et al. (76) assigned the value m = 0.58.

Two authors (45, 46) related the capacity coefficient in gas absorption to a power of the liquid flow rate. That is, $k_L a = HL^P$ where H and P are functions of the packing size and liquid properties.

Sherwood and Holloway (56, 57) present the absorption capacity coefficient as a function of the Reynolds number and the Schmidt number. A similar correlation for the mass transfer coefficient was given by Shulman et al. (58).

Ulbrich and Wild (44) developed a model for absorption of a gas by a liquid flowing in a thin laminar film over defined shapes. Although no data are presented, the model

Reproduced with permission of the copyright owner. Further reproduction prohibited without permission.

reputedly extends the theory of gas absorption into the low liquid flow rate region where the degree of saturation could not be predicted by the penetration theory.

Ammonia absorption and oxygen desorption mass transfer coefficients were correlated by Reiss (49). The author's correlation is based on the concept of energy dissipation per unit volume. Data is fitted within $\pm$ 50%.

Heat and mass transfer factors for the flow of fluids through fixed and fluidized beds of spherical particles are presented by Gupta and Thodos (25). Gas and liquid film mass transfer coefficients are calculated from the Reynolds number, the Schmidt number, and fluid properties. Pelossof (47, 52) calculates mass transfer coefficients for the transport of hydrogen across a thin liquid film. The coefficients are presented as functions of the liquid volumetric flow rate for flow over spheres.

Many of the correlating forms for gas film mass transfer coefficients are similar to those for liquids in that the mass transfer coefficient is presented as a function of the Reynolds numbers and Schmidt numbers. The interested reader is referred to several articles (25, 45, 49, 58, 73).

E. Diluted Catalyst Beds

Since a diluted catalyst bed was employed in the present study, it was felt that a short review of the literature on this subject would be helpful.

Reproduced with permission of the copyright owner. Further reproduction prohibited without permission.

Three pertinent references were chosen for discussion (11, 67, 77). van den Bleek et al. (67) develop a stochastic model of a packed bed reactor with catalyst dilution which shows the influence of dilution on reactor conversion. A dilution criterion is introduced which makes it possible to determine the extent of dilution and the minimum amount of catalyst required to produce a given conversion. No experimental data is presented.

Wilson and Geankoplis (77) demonstrated that dissolution mass transfer coefficients were not affected by diluting the packed bed by a factor of ten-to-one with inert spheres.

Calderbank et al. (11) applied the diluted catalyst fixed bed reactor to exothermic catalytic reactions. The purpose of the dilution was to achieve a particular optimum reaction temperature profile. Examples of the use of the technique were presented by analysis of literature and commercial data. The authors showed that, in many cases, diluted catalyst reactors are small in size, stable in operation, and have a high thermal efficiency.

Reproduced with permission of the copyright owner. Further reproduction prohibited without permission.

CHAPTER II

EQUIPMENT AND OPERATING PROCEDURE

A. Equipment

A trickle-bed reactor was designed and built to study the kinetics of the hydrogenation of alpha-methylstyrene to cumene (isopropylbenzene). Figure II-1 is a schematic diagram of the reactor and its supporting equipment. A more detailed description of the trickle-bed reactor is shown in Figure II-2.

Commercial grade hydrogen of 99.94% purity was fed to the reactor from pressurized cylinders. All gas lines were constructed of clean, dehydrated one-quarter inch copper tubing. After passing through the constant temperature bath, the hydrogen was exposed to a ten inch bed of $CaSO_4$ indicating desiccant to remove any water from the hydrogen. A Matheson Model 70-B low pressure pancake regulator then reduced the line pressure to about seven inches of water. This pressure was chosen so that the reactor would operate at a slight positive pressure to prevent oxygen from leaking into the system. The hydrogen was passed through a rotameter and then fed to the top of the reactor. After

Reproduced with permission of the copyright owner. Further reproduction prohibited without permission.

Reproduced with permission of the copyright owner. Further reproduction prohibited without permission.

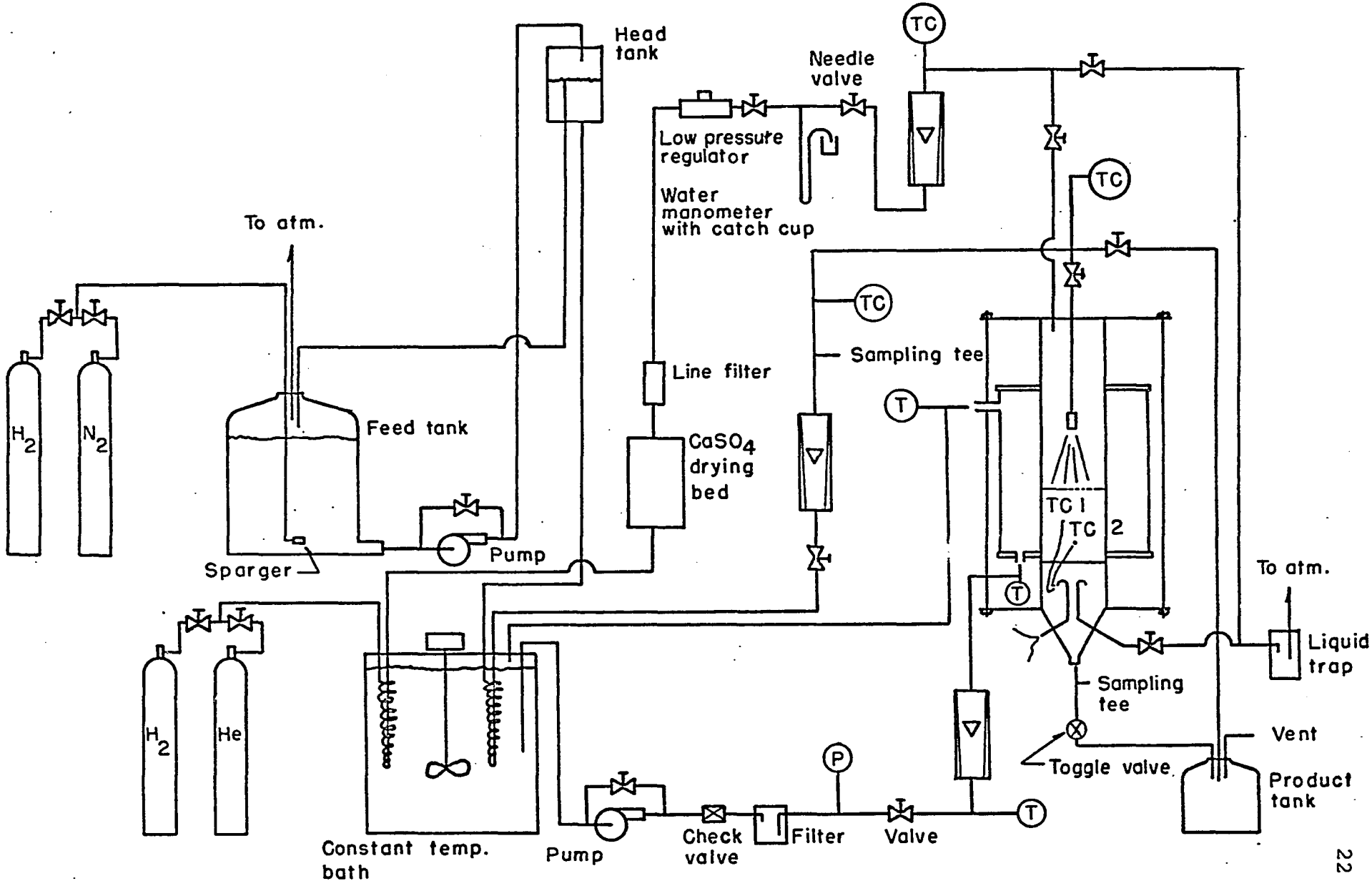

Figure II-1. Flow Diagram of Apparatus

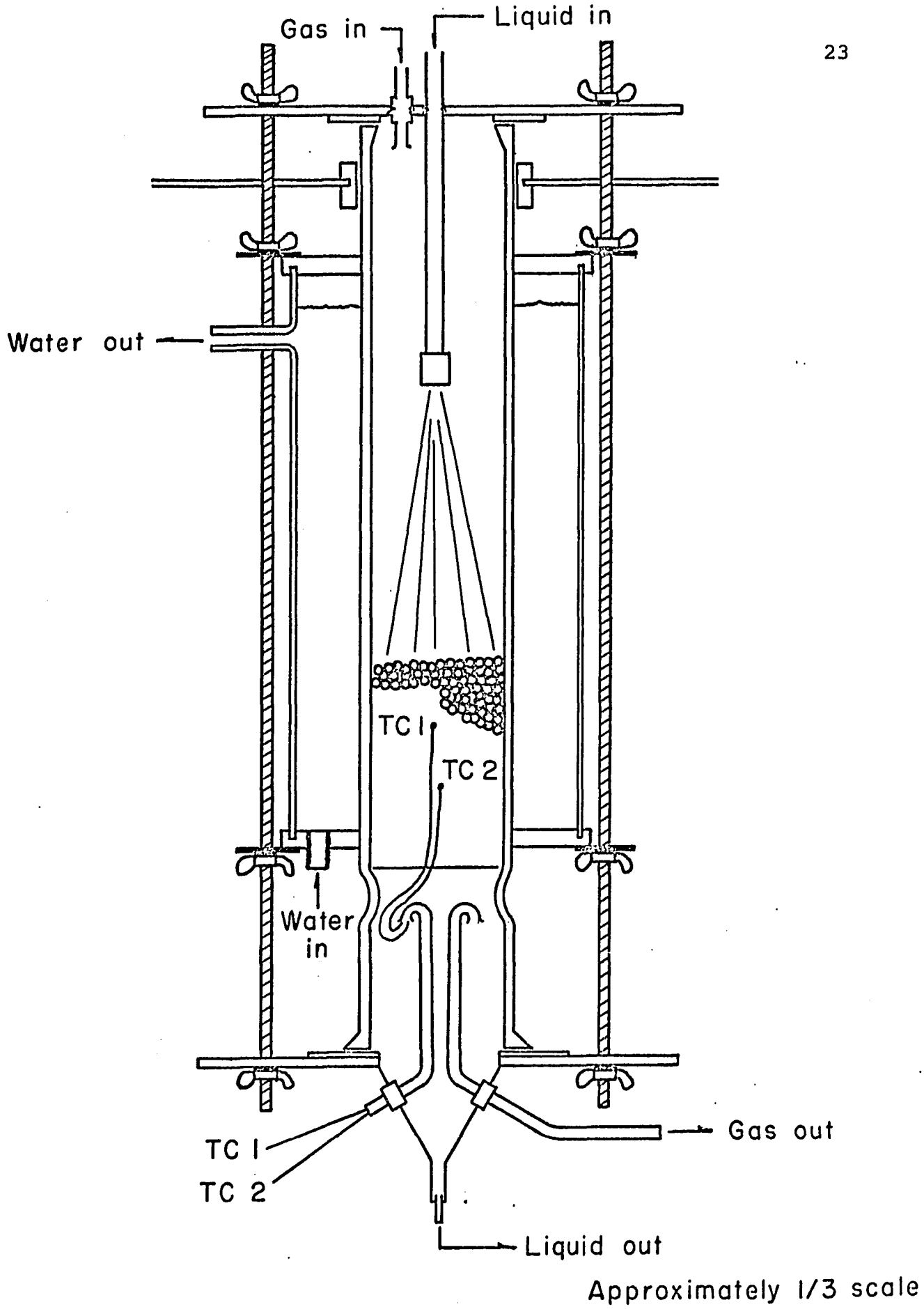

Figure II-2. Schematic Diagram of Trickle-Bed Reactor

Reproduced with permission of the copyright owner. Further reproduction prohibited without permission.

the gas was removed from the bottom of the reactor, it was passed through a liquid trap and exhausted to the atmosphere.

Since alpha-methylstyrene will chemically attack or dissolve many polymers and rubber compounds, it was decided to use only glass, Teflon, and metals in equipment parts which contacted the liquid. Accordingly, all bottle plugs were machined from solid Teflon and Teflon and glass tubings were employed whenever possible. Dehydrated copper tubing was used in the heat exchange coils in the constant temperature bath. Copper tubing was also sparingly used at the liquid feed pump and in lines both entering and leaving the reactor. A five gallon Pyrex bottle with a glass nipple protruding from the side near the bottom served as the feed tank. Liquid was pumped to a head tank thirteen feet above the floor and the majority of it was returned by gravity to the feed tank. A small amount of the liquid passed from the head tank, through the constant temperature bath, to a rotameter equipped with a small needle valve. A liquid sample could be removed at a point just downstream from the rotameter. The liquid then proceeded to the top of the reactor where a small stainless-steel full-jet spray nozzle distributed it evenly over the packing. The product solution was sampled just after leaving the reactor and then

Reproduced with permission of the copyright owner. Further reproduction prohibited without permission.

collected in a two gallon glass bottle. All liquid lines from the constant temperature bath to the reactor were wrapped with insulating tape to reduce heat losses.

The constant temperature bath was actually a converted viscosity bath of eight gallons capacity. The bath was heated by two immersion heaters, one of 0 to 500 watts and the other of 500 to 1000 watts power, and was cooled by tap water circulated through a stainless-steel cooling coil. The water in the bath was controlled within $\pm$ 0.1^{o} F. In order to inhibit rust formation, sodium chromate was added to the water to produce approximately a 0.1% solution. The bath water was circulated at two gallons per minute through the jacket of the reactor to control the reaction temperature. All water lines were constructed of white brass and insulating tape was used where necessary to minimize heat losses.

The trickle-bed reactor was constructed of a 24 inch length of medium wall Pyrex glass tubing with an inside diameter of three inches. A crimp in the glass four inches from the bottom of the reactor served as a support for the perforated aluminum disc which held up the packed bed. Concentric to this inner tubing was a sixteen inch length of Pyrex tubing with an outer diameter of 5.5 inches. The outer shell was restrained by two Plexiglas flanges and the volume between the two shells served as the reactor

Reproduced with permission of the copyright owner. Further reproduction prohibited without permission.

jacketing. Flanges at the top and bottom of the reactor were machined of 3/16 inch brass and were clamped together by four 28 inch long threaded rods. The system was well sealed by a Teflon envelope gasket at each end of the reactor between the brass plate and the end of the glass tubing. A three inch diameter stainless-steel funnel was soldered to the bottom of the lower brass plate. This funnel collected the liquid phase effluent from the reactor. In addition, through two holes in the sides of the funnel two pieces of copper tubing were extended about two inches into the reactor. One tube carried the gas phase (hydrogen) from the reactor while the other tube provided a simple means of introducing two thermocouples into the bottom of the packed bed. A small full-jet spray nozzle with an angle of spray of 25^{o} was chosen as the liquid distributor for the top of the reactor. The full-jet spray nozzle distributed the liquid evenly in a circular pattern across the entire top layer of packing. The nozzle was positioned about 8 inches down from the brass plate and about 7 inches above the top of the packing in order to provide a good liquid distribution on the top of the bed. Care was taken to position the column exactly vertical prior to each run. This was done by adjusting three restraining arms on the outside of the reactor near the top.

Reproduced with permission of the copyright owner. Further reproduction prohibited without permission.

The catalyst employed was manufactured by the Houdry Process and Chemical Company (details of the manufacturing process and properties of the catalyst and the reactor bed are given in Table B-1 of Appendix B). The catalyst consisted of 0.3 weight percent palladium deposited on the surface of the non-porous mineral, dolomite. The irregularly shaped granules (of both active catalyst and inert dolomite) had a size distribution of 10-16 mesh, which corresponded to an average equivalent sphere diameter of 1.61 millimeters.

Commercial grade alpha-methylstyrene and cumene were used as received from the Dow Chemical Company. The alpha-methylstyrene was about 99.45% pure, the 0.55% impurity being normal-propyl benzene. A trace of cumene (0.03%) was also present in the alpha-methylstyrene.

B. Operating Procedure

After the equipment had been completely assembled and checked for leaks, approximately ten runs were conducted to establish procedures of operation. It was first demonstrated that there was no homogeneous reaction and that neither the glass walls of the reactor nor the inert dolomite packing catalyzed the reaction. Secondly, it was found that 600 grams of inert dolomite mixed with 100 grams of active

Reproduced with permission of the copyright owner. Further reproduction prohibited without permission.

catalyst was a good dilution ratio in that a measurable conversion could be obtained without a severe temperature rise through the bed. The actual temperature increase amounted to about 1.0° C per one percent conversion. Across a "differential bed" of 100 grams of active catalyst, the temperature rose about 3° C per one percent conversion (6). By placing one thermocouple near the reactor wall and the other on the bed centerline, it was established that radial temperature gradients were negligible even at the lowest liquid flow rates employed. Also, due to heat losses from the transport lines, the bath temperature did not exactly correspond to the jacket or the reactor temperature. Therefore, a rough correlation was developed between the bath temperature and the desired reaction temperature.

Once these preliminary experiments were completed, the useful experimental portion of the research was begun. The operational procedure for a typical run from numbers 7 through 25 is presented.

About two hours before an experiment was begun, the controllers of the constant temperature bath and the gas chromatograph were turned on to allow them time to heat up and equilibrate. During this interval, the reactor was vertically positioned in its stand. For Runs 7, 9, and 18 new catalyst beds were prepared by weighing out and gently

Reproduced with permission of the copyright owner. Further reproduction prohibited without permission.

mixing 100 grams of active catalyst with 600 grams of inert dolomite. Runs 8 and 10 through 17 reused the catalyst from Run 7, while Runs 18 through 25 employed the catalyst prepared for Run 18. The two thermocouples were then held in position on the bed centerline and the aluminum bed-support disc was placed on its holders. About 150 grams of the mixed catalyst was then poured over the aluminum plate. This depth of packing (approximately one inch) was lightly tapped for 20 seconds with a 1/8 inch glass rod. The tapping was done to minimize shifting of particles in the bed when liquid was dropped onto it and to give a reproducible bed density. The catalyst bed was completely packed after four or five pourings of packing material with intermittent tapping. At this point the bed was 4-1/2 inches high with thermocouples positioned on the centerline 1-1/8 inches and 2-1/2 inches from the bottom of the bed. The water was then circulated through the reactor jacketing to bring the bed temperature to the operating level. Two and one-half to five gallons of alpha-methylstyrene were poured into the feed tank. The bottle was sealed and was purged with nitrogen gas. The reactor was also sealed, tested for leaks, and then purged with helium. The catalyst bed was reduced with hydrogen for fifteen minutes. Complete reduction apparently took place within five minutes after hydrogen

Reproduced with permission of the copyright owner. Further reproduction prohibited without permission.

was initially fed to the reactor. Evidence of this effect was given by a color change from brown palladium oxide to black palladium metal the first time the catalyst was reduced. On reoxidation, however, the palladium did not revert back to the brown color. The feed liquid was circulated through its transport lines to preheat them to the operating temperature. At this time a sample of liquid feed was taken and analyzed in the gas chromatograph (a detailed description of the chromatographic analysis is given in Appendix A). After all temperatures were equilibrated and the bed was reduced, the alpha-methylstyrene was admitted to the bed. The time of this event was recorded as time zero for the experiment. Liquid product samples were withdrawn and analyzed in the gas chromatograph every two to five minutes depending upon the conditions of the experiment. At the same time, temperatures were measured with the aid of thermocouples and a potentiometer. After three to seven minutes (depending upon the liquid flow rate) the visible portions of the catalyst bed were completely wetted. Runs in this series lasted anywhere from twenty to ninety minutes. A run was terminated after the conversion passed through its maximum and was falling off at a reasonably slow, constant rate. A liquid feed sample was taken at the end of the run to determine if an

Reproduced with permission of the copyright owner. Further reproduction prohibited without permission.

appreciable change in feed composition occurred during the run. The hydrogen was then turned off and helium was fed to the reactor. Alpha-methylstyrene flowed through the reactor for an additional three or four minutes and then its flow was also terminated. Flow of water to the jacket was stopped and the water was returned to the bath. The catalyst bed was removed and air-dried for at least 24 hours. The inside reactor wall was cleaned and the excess alpha-methylstyrene was drained from its transport lines.

Runs 26, 27, and 28 employed the same catalyst bed and reactor temperature as in Runs 18 through 25. However, the operating procedure was changed slightly. The changes were made because it was felt that the decrease in catalyst activity with time might have been a result of air-drying between runs or of abrasive removal of palladium from the catalyst surface in handling the packing between runs. In addition, there was the possibility that local variations in the bed packing and wetting characteristics would produce significant changes in the bed-average conversion. Packing and re-packing a bed might then lead to non-comparable results. The modified procedure was basically identical to that discussed before except that the order of addition of the reactants to the reactor was changed. The alpha-methylstyrene was admitted to the bed first. After the bed

Reproduced with permission of the copyright owner. Further reproduction prohibited without permission.

was completely wetted, the hydrogen was fed to the reactor. The shut-down procedure was unchanged except that the bed was left wetted with alpha-methylstyrene and in contact with helium between runs.

Runs 30 through 37 employed the modified operating procedure, the reactor temperature being 40° C. New catalyst was made up for Run 30 and was used through Run 37.

A catalyst concentration of 50 grams of catalyst to 650 grams of inert dolomite was used in Run 38. For Run 39, the ratio was 200 grams of active catalyst to 500 grams of dolomite. However, the operating procedure was unchanged for these runs.

In an effort to prove that both new catalyst activity and the catalyst deactivation rate were repeatable from one batch of catalyst to the next, Run 40 was conducted for a continuous four hour period. The catalyst dilution ratio (using new catalyst) was 100/600 and the modified operational procedure was employed.

Reproduced with permission of the copyright owner. Further reproduction prohibited without permission.

CHAPTER III

RESULTS

Alpha-methylstyrene is converted to cumene by the addition of hydrogen over a palladium catalyst. A review

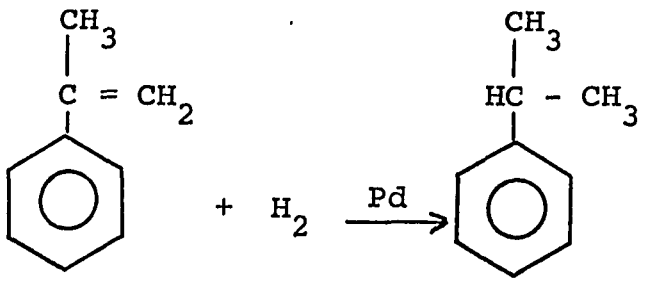

$$\Delta H_R = -25{,}250 \ \frac{\text{cal.}}{\text{gm. mole}}$$

of the literature indicates that palladium supported on alumina pellets was most often used as the catalyst (6, 34, 40, 47, 52), although palladium black was employed in one research program (20, 55). With a palladium catalyst, cumene is the only product formed and the reaction proceeds to completion at the conditions used in the present experimental program (34). Alpha-methylstyrene and cumene have very low vapor pressures at room temperature, the values being 2.7 mm. Hg. at 25° C and 5.0 mm. Hg. at 26.8° C, respectively. Therefore the vapor phase of the reactor at one atmosphere total pressure is essentially all hydrogen.

In the present investigation the catalyst employed was 0.3 weight percent palladium deposited on the surface of

Reproduced with permission of the copyright owner. Further reproduction prohibited without permission.

10-16 mesh irregular dolomite granules. Dolomite is essentially non-porous and therefore the reactive surface area is only the external surface area of the catalyst.

It was necessary to conduct some preliminary tests on the catalyst, the inert dolomite, and the reactor itself before proceeding with trickle-bed experiments. The palladium-on-dolomite catalyst was quickly and quantitatively reduced by hydrogen at room temperature and one atmosphere pressure. The reduction was characterized by a color change from brown (palladium oxide) to black (palladium metal) and was thus plainly visible. The catalyst selectively converted the alpha-methylstyrene to cumene without saturating any part of the benzene ring. This result is in agreement with the findings of other researchers (6, 47, 52). In a catalyst free reactor it was demonstrated that no homogeneous reaction occurred and that no parts of the reactor or the supporting equipment catalyzed the reaction. Similarly, the inert dolomite did not promote the reaction. No previous investigators have reported any polymer formation at these mild conditions. Literature data (5) indicate that polymer formation should be minimal below 200° C. Even at 250° C only small amounts of unsaturated dimer and trimer are formed (5). Viscosity measurements of the feed and product liquids indicated that no polymer was formed in the present

Reproduced with permission of the copyright owner. Further reproduction prohibited without permission.

study. The same conclusion was reached when no solids precipitated from the product solutions on the addition of large volumes of methanol. Preliminary experiments indicated that 100 grams of catalyst were necessary to produce a maximum of about 5% conversion at the conditions employed. A dilution ratio of 100 grams of active catalyst to 600 grams of inert dolomite was used in all runs except numbers 38 and 39. Good temperature control was achieved by using this dilution ratio. Table B-1 in Appendix B presents information on the catalyst and the reactor bed conditions.

With the preliminary experiments completed, a program was initiated to determine the effects of process variables on the extent of conversion. The parameters studied were liquid and gas flow rates, bed temperature, and, to a lesser extent, catalyst weight. A summary of the conditions used in each run is given in Table B-2 in Appendix B. Since it was observed that the catalyst deactivated due to poisoning during usage, it was also necessary to study the poisoning effect. The results of the effects of each of these variables is discussed individually. Since the effects of all other process variables were dependent upon an analysis of the deactivation phenomenon, the poisoning effect is discussed first.

Reproduced with permission of the copyright owner. Further reproduction prohibited without permission.

A. Effect of Poisoning

Early in the experimental program it was noticed that catalyst deactivation was occurring. This was observed when attempts failed to produce repeatable results from run to run on the same catalyst. For example, Runs 7, 8, and 10 were all made at identical liquid and gas flow rates and at the same temperature on a single catalyst bed. However, at comparable times during each run, the conversion always fell below that of the previous run. Subsequent analysis of the data showed that the catalyst was deactivated at a rate which was exponentially dependent upon the total time of catalyst use, the process time τ. The exponential relationship between the reaction rate, r, and τ is shown in Figures III-1, III-2, and III-3 at the three temperatures 32° C, 40° C, and 50° C, respectively. Each datum point represents the result of a single run; the reaction rate was calculated from the conversion at that time. The reaction rate was then plotted against the total time of catalyst usage (τ) on semilogarithmic paper. The straight lines on each of Figures III-1, III-2, and III-3 represent the best statistical fit of all of the points at each temperature. An OMNITAB program employing the least squares method of data analysis was used to develop the best fit.

Reproduced with permission of the copyright owner. Further reproduction prohibited without permission.

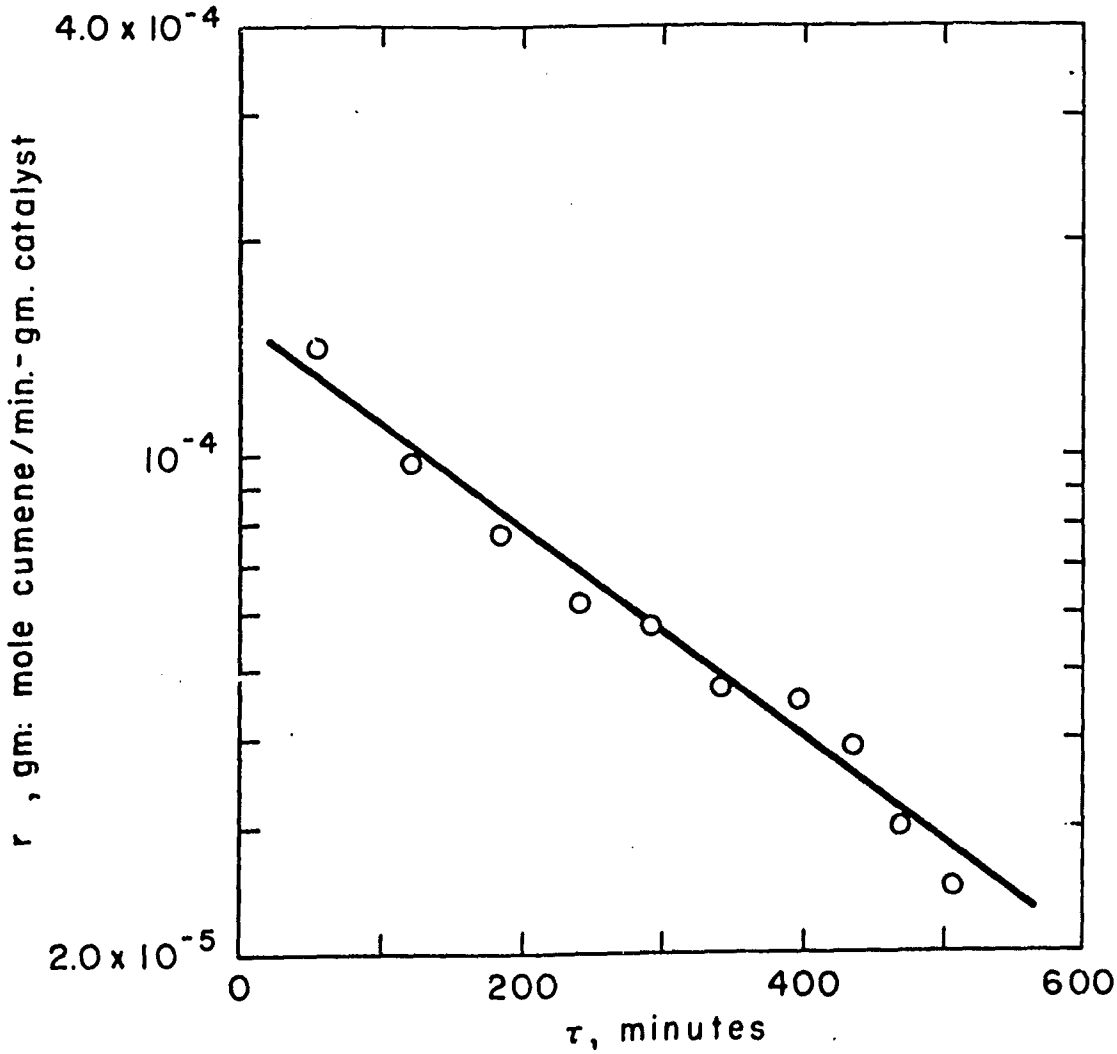

Figure III-1. Reaction Rate as a Function of Process Time at 32° C

Reproduced with permission of the copyright owner. Further reproduction prohibited without permission.

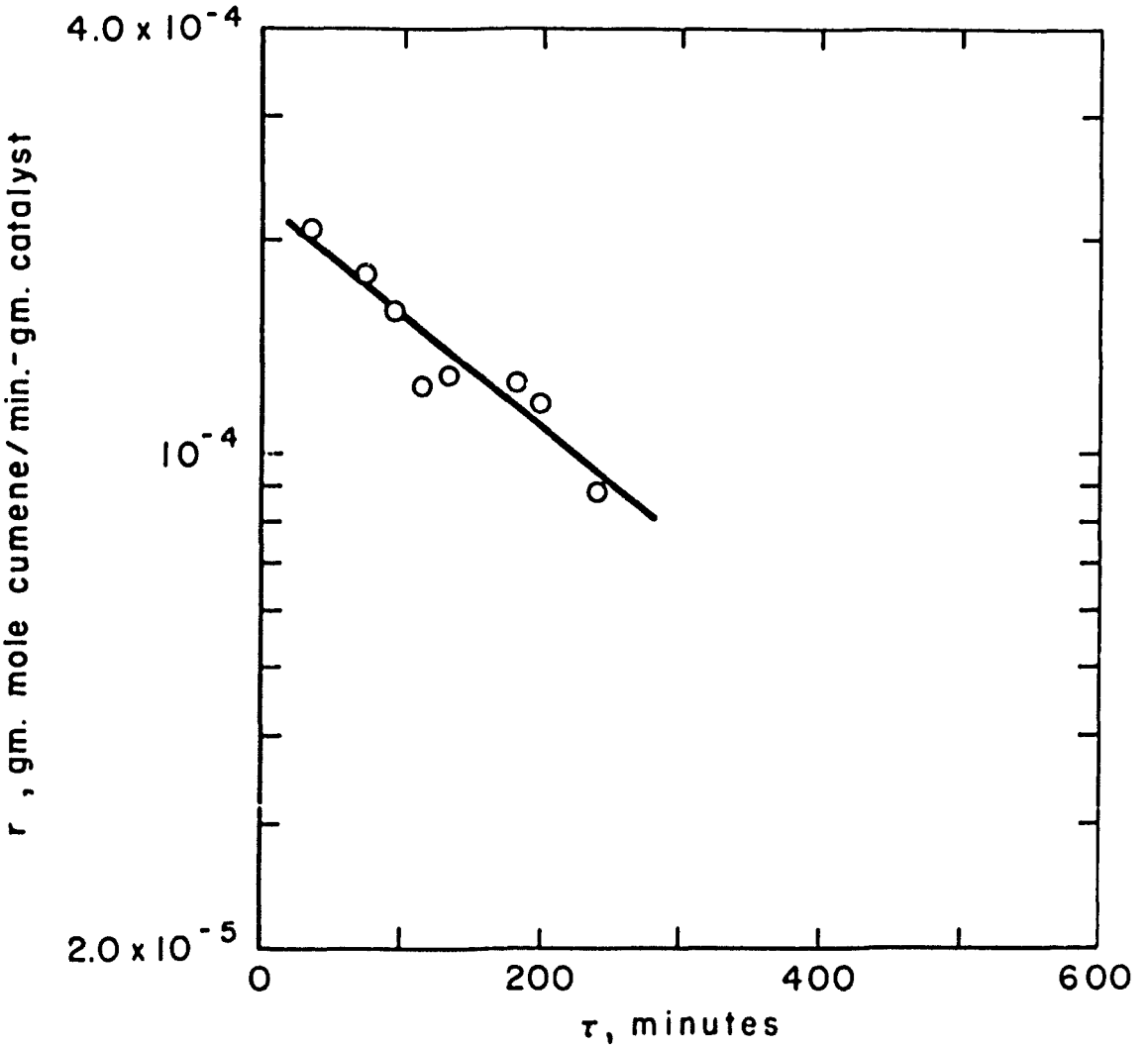

Figure III-2. Reaction Rate as a Function of Process Time at 40° C

Reproduced with permission of the copyright owner. Further reproduction prohibited without permission.

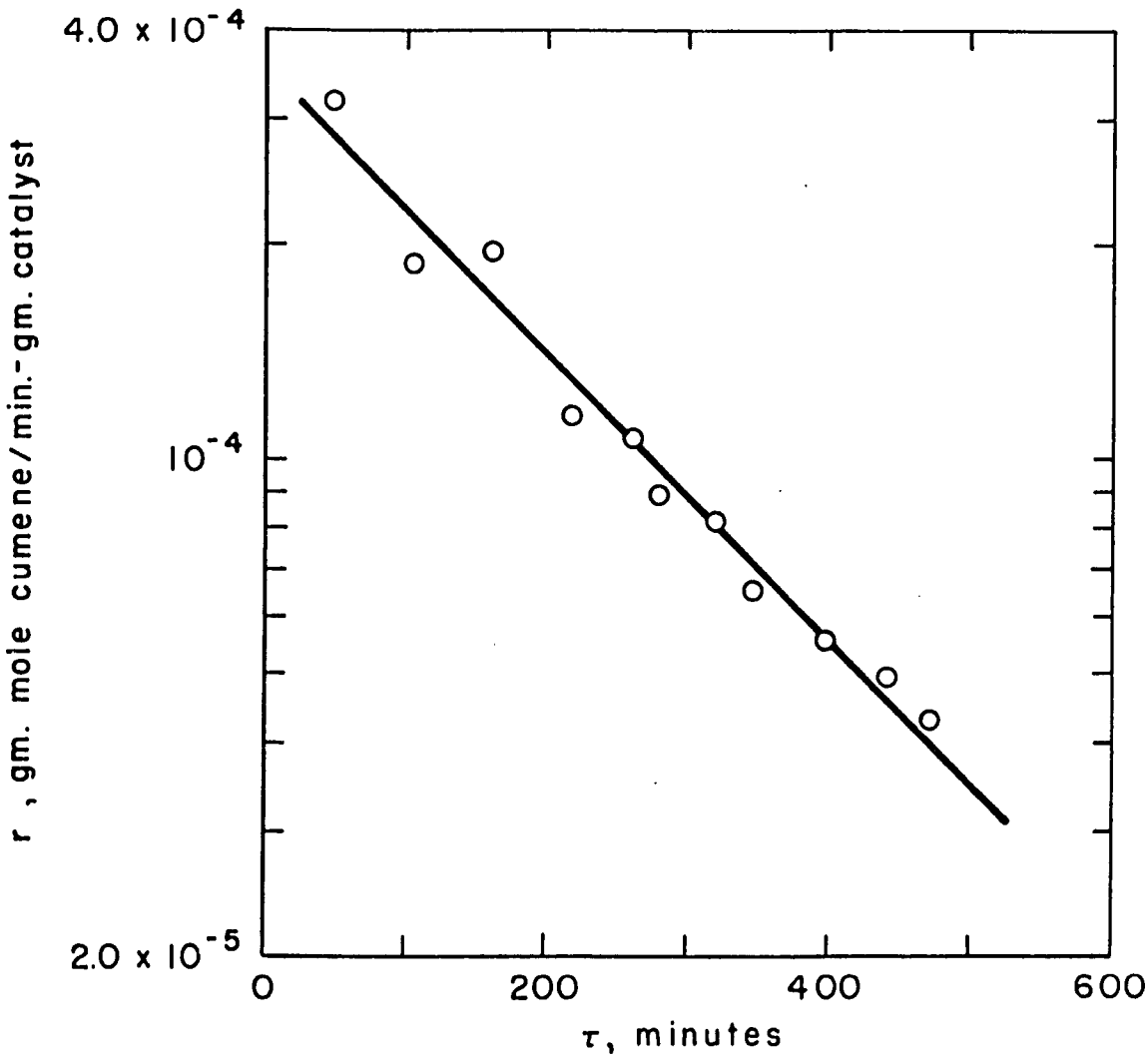

Figure III-3. Reaction Rate as a Function of Process Time at 50° C

Reproduced with permission of the copyright owner. Further reproduction prohibited without permission.

The equations of the best lines through the data and the standard deviations of the curves are as follows:

at 32^{o} C

$$\ln r = -8.77 - 3.45 \times 10^{-3} \tau \quad , \sigma = 9.00 \times 10^{-2}$$

at 40^{o} C

$$\ln r = -8.40 - 3.72 \times 10^{-3} \tau \quad , \sigma = 1.03 \times 10^{-1}$$

at 50^{o} C

$$\ln r = -7.95 - 4.62 \times 10^{-3} \tau \quad , \sigma = 1.08 \times 10^{-1}$$

These equations are of the form,

$$\ln r = \ln r_{o} - \alpha\tau \qquad \text{(III-1)}$$

where α is a constant (at a given temperature) which increases slightly with increasing temperature. Since r_{o} represents the reaction rate of a fully active catalyst ($\tau = o$), then Equation (III-1) is equal to,

$$r = k_{o} C^{*} e^{-\alpha\tau} = k_{o} C^{*} \phi \qquad \text{(III-2)}$$

Using Equation (III-2) k_{o} was calculated for each datum point. The value of α used at each temperature was the one determined from the best fit through all the points. The results are presented in Tables III-1, III-2, and III-3. This procedure for calculating k_{o} for each run should be justified in that the extrapolation to zero time is over a relatively short time period, 30 to 60 minutes in the three cases.

Reproduced with permission of the copyright owner. Further reproduction prohibited without permission.

TABLE III-1

REACTION RATE DATA AT 32° C

Run Number	$r \times 10^{+5}$ $\left(\frac{\text{gmoles cumene}}{\text{min. - gm. cat.}}\right)$	$\phi = e^{-\alpha\tau}$	k_o $\left(\frac{\text{cc. liquid}}{\text{sec. - gm. cat.}}\right)$
7	14.2	0.827	0.925
8	9.75	0.658	0.796
10	7.76	0.529	0.789
11	6.17	0.434	0.762
12	5.77	0.367	0.843
13	4.70	0.308	0.820
14	4.50	0.254	0.953
15	3.90	0.223	0.940
16	3.00	0.198	0.814
17	2.47	0.174	0.763
			$\bar{k}_o = 0.8405$

$$\ln r = -8.77 - 3.45 \times 10^{-3} \tau$$

$$k_o = \frac{r}{e^{-\alpha\tau} C^*}$$

$$C^* = 3.1 \times 10^{-6} \text{ gmoles } H_2\text{/cc. liquid}$$

$$\bar{k}_o = 0.841 \pm 0.073$$

Reproduced with permission of the copyright owner. Further reproduction prohibited without permission.

TABLE III-2

REACTION RATE DATA AT 40° C

Run Number	$r \times 10^{+5}$ $\left(\frac{\text{gmoles cumene}}{\text{min. - gm. cat.}}\right)$	$\phi = e^{-\alpha\tau}$	k_o $\left(\frac{\text{cc. liquid}}{\text{sec. - gm. cat.}}\right)$
30	20.8	0.861	1.22
31	17.9	0.763	1.18
32	15.8	0.702	1.135
33	12.4	0.660	0.948
34	12.8	0.615	1.05
35	12.6	0.508	1.25
36	11.7	0.477	1.235
37	8.80	0.411	1.08
			$\bar{k}_o = 1.137$

$$\ln r = -8.40 - 3.72 \times 10^{-3} \tau$$

$$k_o = \frac{r}{e^{-\alpha\tau} C^*}$$

$$C^* = 3.3 \times 10^{-6} \text{ gmoles } H_2/\text{cc. liquid}$$

$$\bar{k}_o = 1.14 \pm 0.11$$

Reproduced with permission of the copyright owner. Further reproduction prohibited without permission.

TABLE III-3

REACTION RATE DATA AT 50° C

Run Number	$r \times 10^{+5}$ $\left(\frac{\text{gmoles cumene}}{\text{min. - gm. cat.}}\right)$	$\phi = e^{-\alpha\tau}$	$k_o \left(\frac{\text{cc. liquid}}{\text{sec. - gm. cat.}}\right)$
18	31.9	0.787	1.93
19	18.7	0.616	1.45
20	19.5	0.475	1.95
21	11.5	0.368	1.49
22	10.7	0.301	1.70
23	8.83	0.275	1.53
24	8.19	0.227	1.71
25	6.49	0.202	1.53
26	5.53	0.159	1.66
27	4.91	0.130	1.80
28	4.27	0.113	1.80
			$\bar{k}_o = 1.686$

$$\ln r = -7.95 - 4.62 \times 10^{-3} \tau$$

$$k_o = \frac{r}{e^{-\alpha\tau} C^*}$$

$$C^* = 3.5 \times 10^{-6} \text{ gmoles } H_2/\text{cc. liquid}$$

$$\bar{k}_o = 1.69 \pm 0.17$$

Reproduced with permission of the copyright owner. Further reproduction prohibited without permission.

In order to demonstrate that the deactivation was indeed occurring at a reasonably constant rate at a given temperature, Run 40 was conducted for a continuous period of almost four hours. The reaction temperature was 32^{o} C. Figure III-4 presents the results of that run in the form of ln r plotted against process time, τ . Points at 6 and 10 minutes are characteristically low due to the start-up procedure and are excluded from the remainder of the analysis. An OMNITAB least squares fit of the data from Run 40 yielded the result,

$$\ln r = -8.68 - 3.73 \times 10^{-3} \tau \ , \ \sigma = 0.0699$$

Due to a temporary failure of the temperature controller in the period between 100 and 140 minutes, the reaction rates during that time were lower than normal. A least squares fit of the data excluding the points between 100 and 140 minutes gave,

$$\ln r = -8.64 - 3.78 \times 10^{-3} \tau \ , \ \sigma = 0.0409$$

Thus, excluding these points from the analysis gave a slightly better overall fit (smaller sigma), but the coefficients in the equation were essentially unchanged.

From this point on in the presentation of the results all reaction rates and rate constants are actually r_o and k_o, the functions which are independent of the catalyst deactivation rate.

Reproduced with permission of the copyright owner. Further reproduction prohibited without permission.

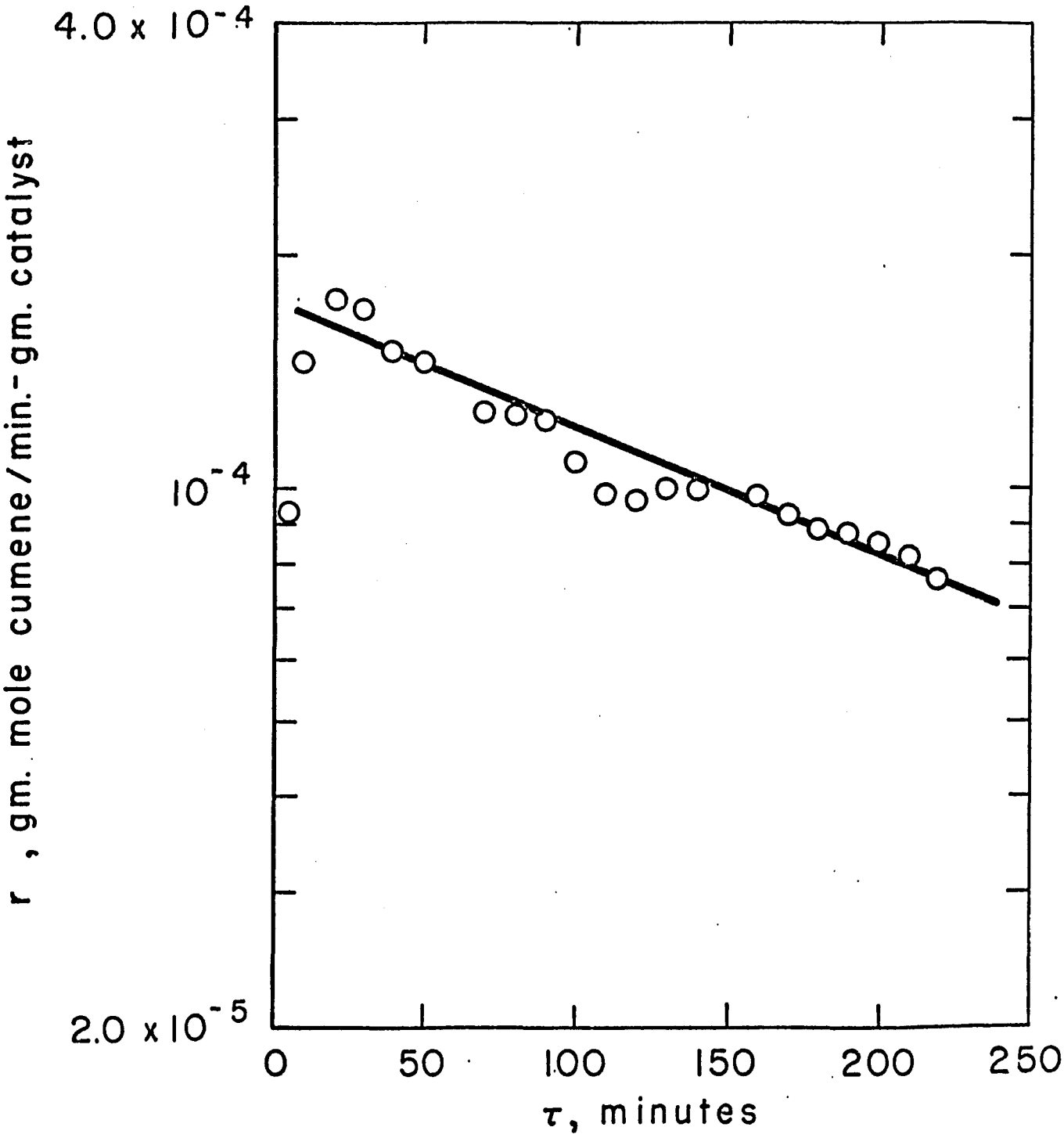

Figure III-4. Reaction Rate as a Function of Process Time for Run 40 at 32° C

Reproduced with permission of the copyright owner. Further reproduction prohibited without permission.

B. Effect of Gas Flow Rate

The hydrogen flow rate was varied between 1.0 liters/minute and 2.5 liters/minute. This corresponded to a Reynolds number range from 0.0481 to 0.136 based on the pellet diameter. Table B-2 in Appendix B summarizes the conditions under which each of the runs was made. A typical plot of the rate constant, k_o, versus the gas flow rate, G, at 50° C and a liquid flow rate of 100 cc/minute is shown in Figure III-5. Figure III-6 is a similar plot except that points are included for all values of the liquid flow rate. Both figures demonstrate that the rate constant at all temperatures is independent of the gas flow rate in the range studied.

C. Effect of Liquid Flow Rate

The liquid feed rates (L) ranged from 100 cc/minute to 225 cc/minute and represented Reynolds numbers from 0.655 to 1.52 based on the pellet diameter. Figure III-7 is a typical plot of k_o versus L at 40° C and a gas flow rate of 1.0 liter/minute. Figure III-8 is the corresponding plot at all values of gas flow rate. Again both plots show that within the experimental error, the rate constant is independent of liquid flow rate over the range employed.

Reproduced with permission of the copyright owner. Further reproduction prohibited without permission.

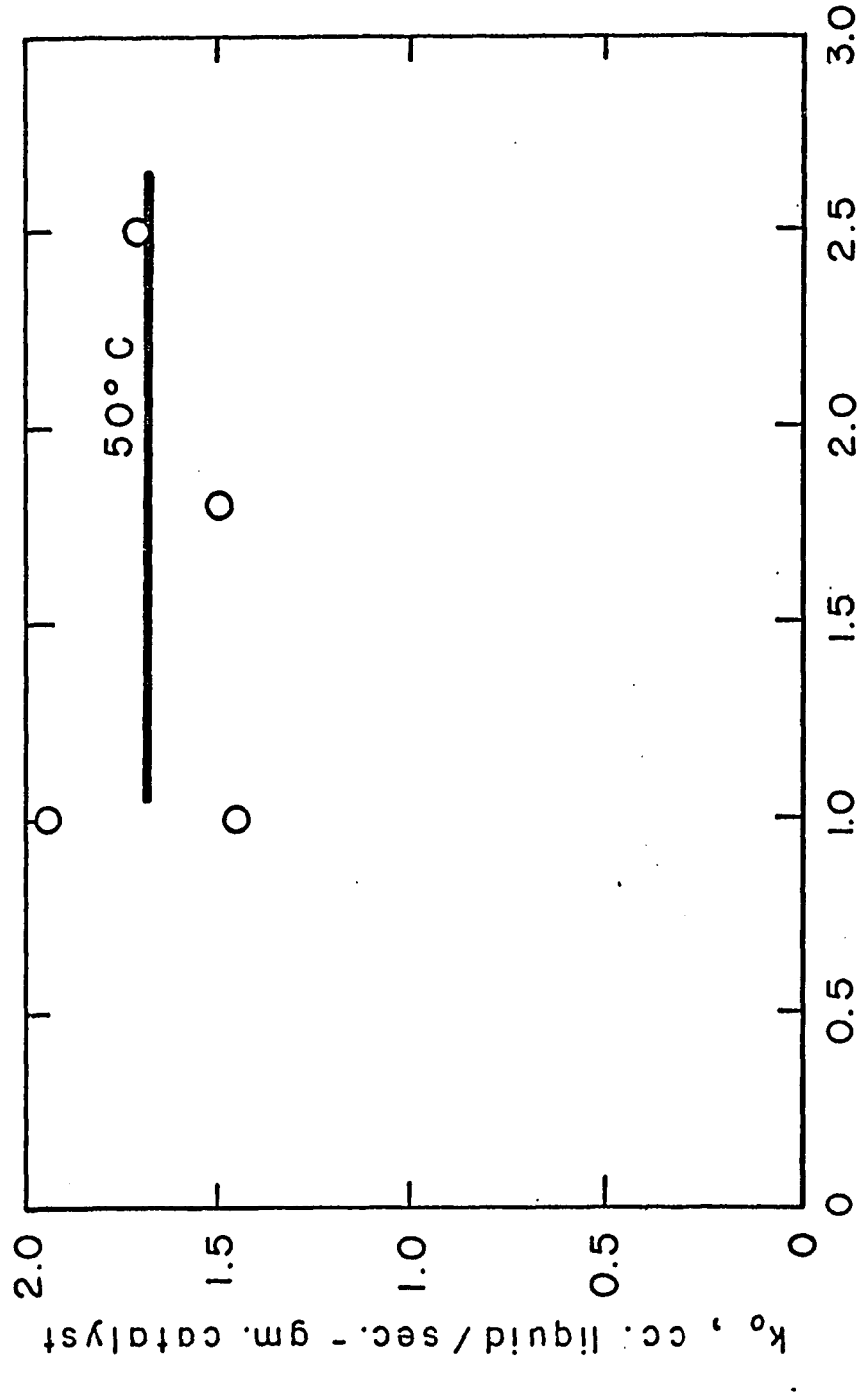

Figure III-5. Effect of Gas Flow Rate on Intrinsic Rate Constant for L = 100 cc./min. at 50° C

Reproduced with permission of the copyright owner. Further reproduction prohibited without permission.

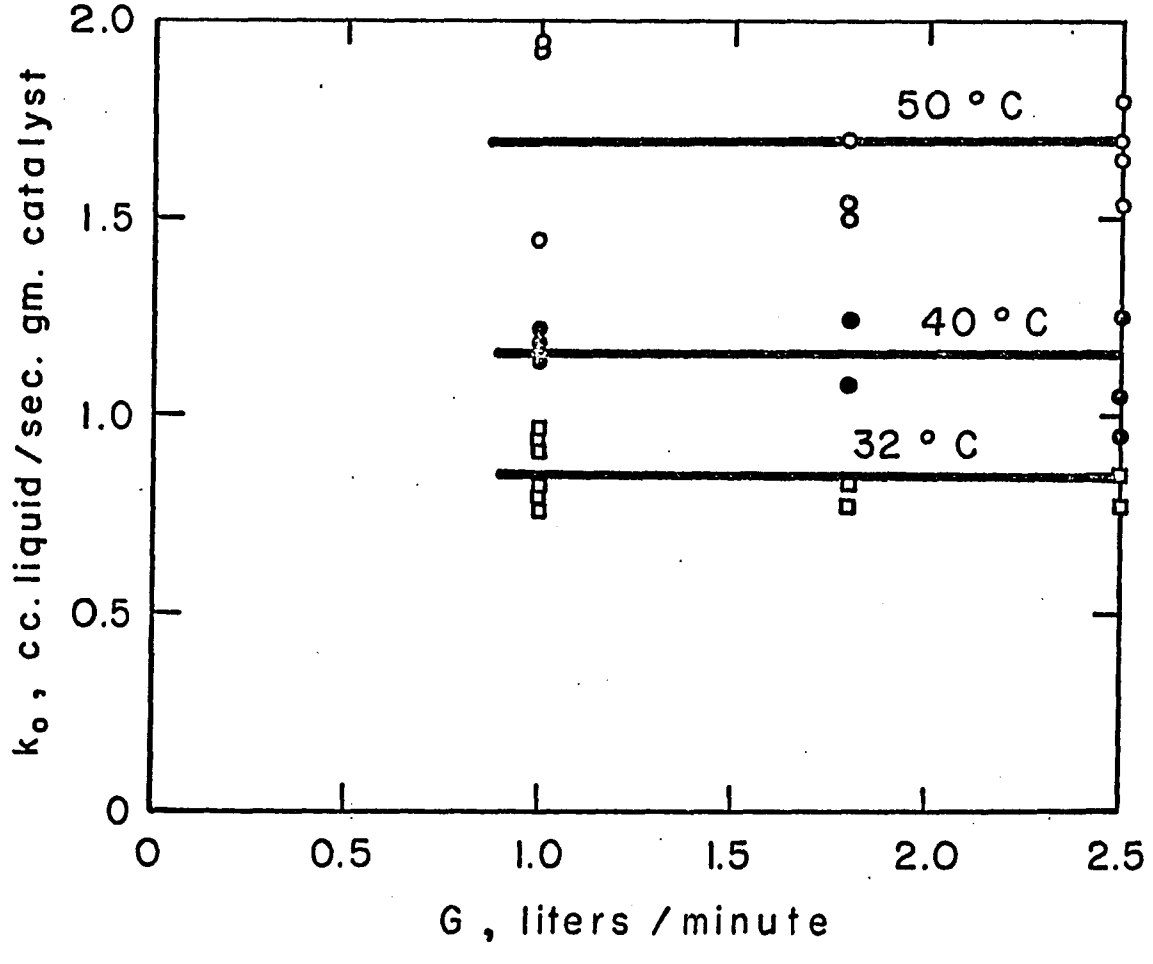

Figure III-6. Effect of Gas Flow Rate on Intrinsic Rate Constant for All Liquid Flow Rates

Reproduced with permission of the copyright owner. Further reproduction prohibited without permission.

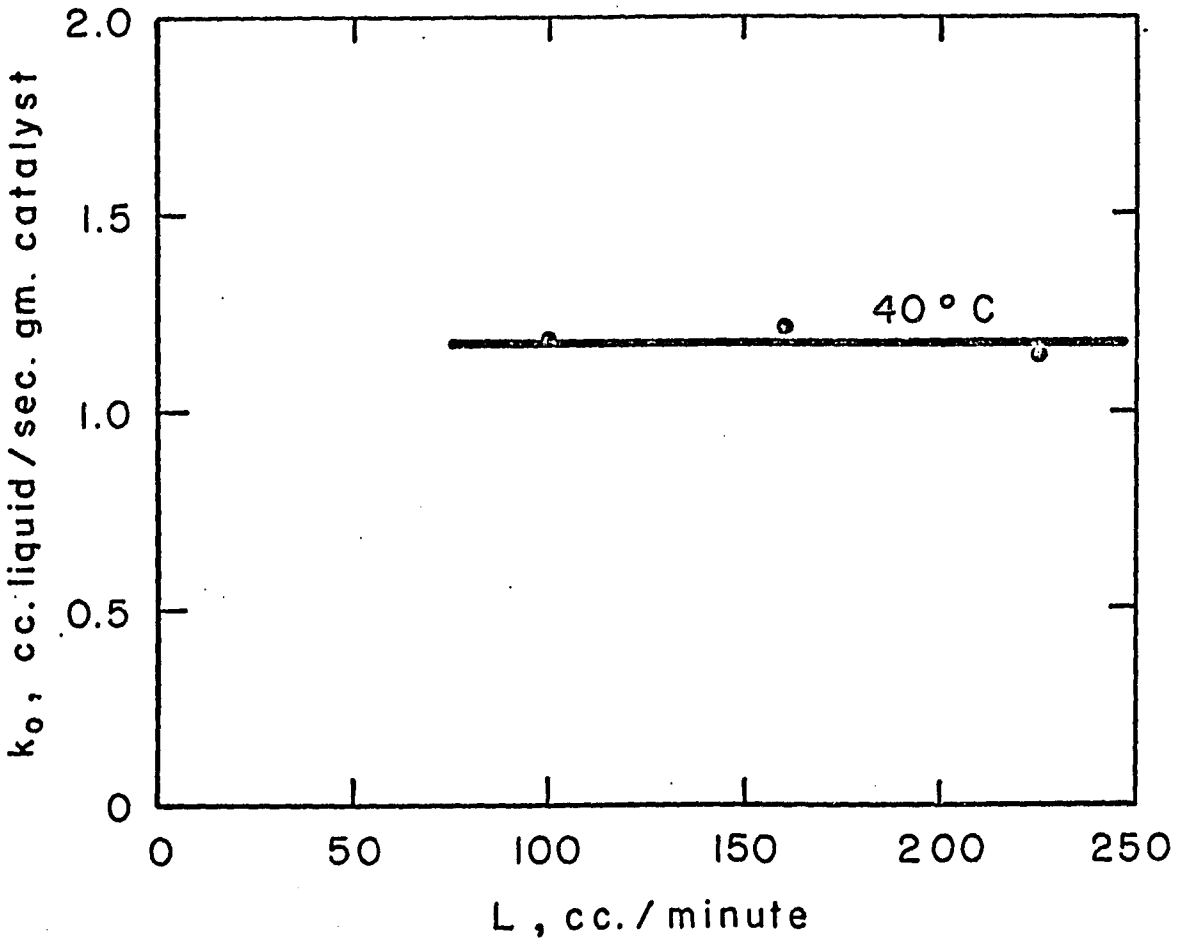

Figure III-7. Effect of Liquid Flow Rate on Intrinsic Rate Constant for G = 1.0 liters/min. at 40° C

Reproduced with permission of the copyright owner. Further reproduction prohibited without permission.

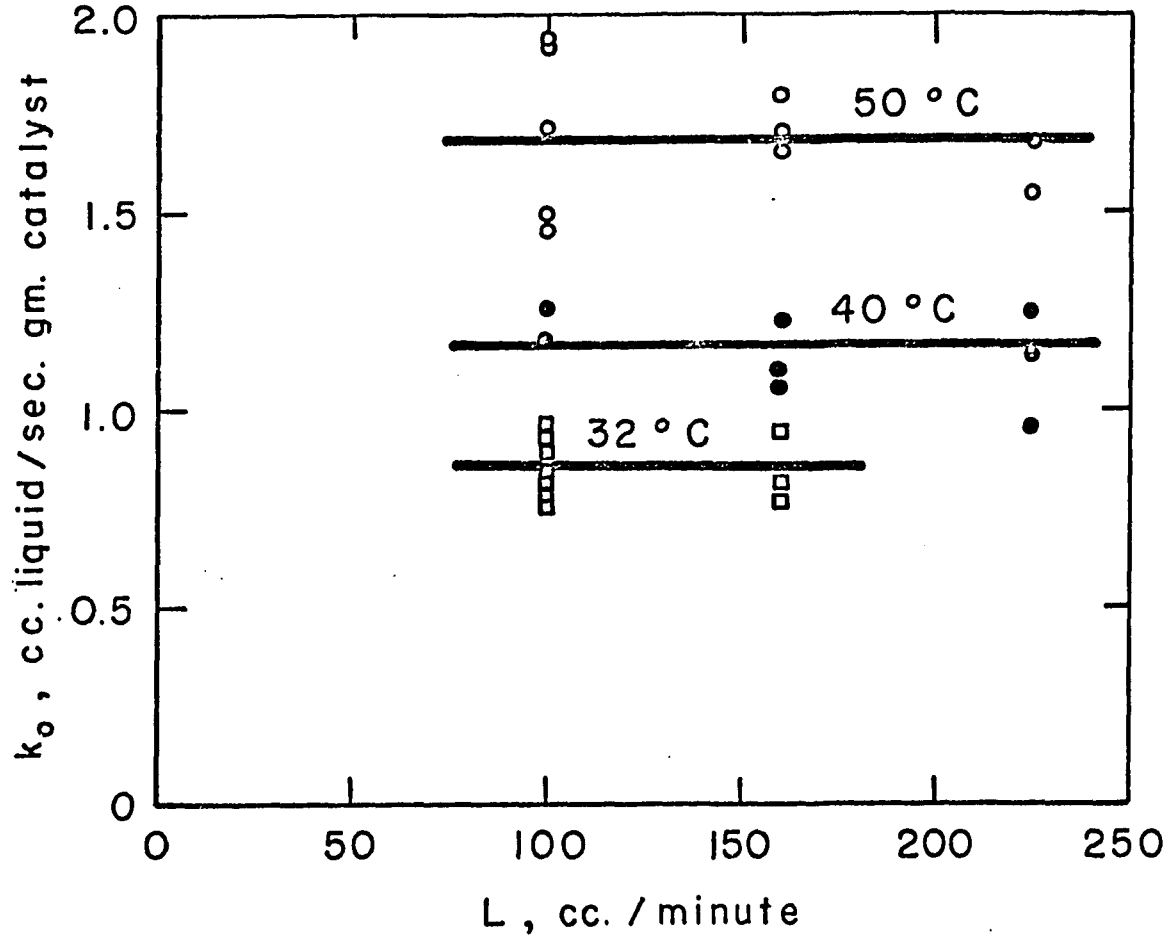

Figure III-8. Effect of Liquid Flow Rate on Intrinsic Rate Constant for All Gas Flow Rates

Reproduced with permission of the copyright owner. Further reproduction prohibited without permission.

D. Effect of Temperature

The effect of temperature on the observed rate constant is quite significant in the range 32° C to 50° C. The rate constant increases exponentially with temperature as shown in Figure III-9. From the slope of the straight line on the Arrhenius plot an activation energy for reaction of 7,280 ± 337 cal./gm.mole was calculated. The effect of temperature on the physical properties of alpha-methylstyrene and hydrogen is given in Figures C-1, C-2, C-3, C-4, and C-5 in Appendix C.

E. Effect of Catalyst Weight

Runs 38 and 39 were conducted to determine the effect of the weight of catalyst on the rate of conversion of alpha-methylstyrene to cumene. Fifty grams of active catalyst were mixed with 650 grams of dolomite in Run 38, while Run 39 used a dilution of 200 grams of catalyst in 500 grams of dolomite. The rate of cumene formation (gm.moles cumene/minute) was calculated from the liquid flow rate and the observed mole fraction of cumene in the product. Conversion data was arbitrarily chosen as the effluent conversion observed at a time of 30 minutes into each run. This time period was chosen because it was long enough to exceed the transient start-up time and yet short enough that

Reproduced with permission of the copyright owner. Further reproduction prohibited without permission.

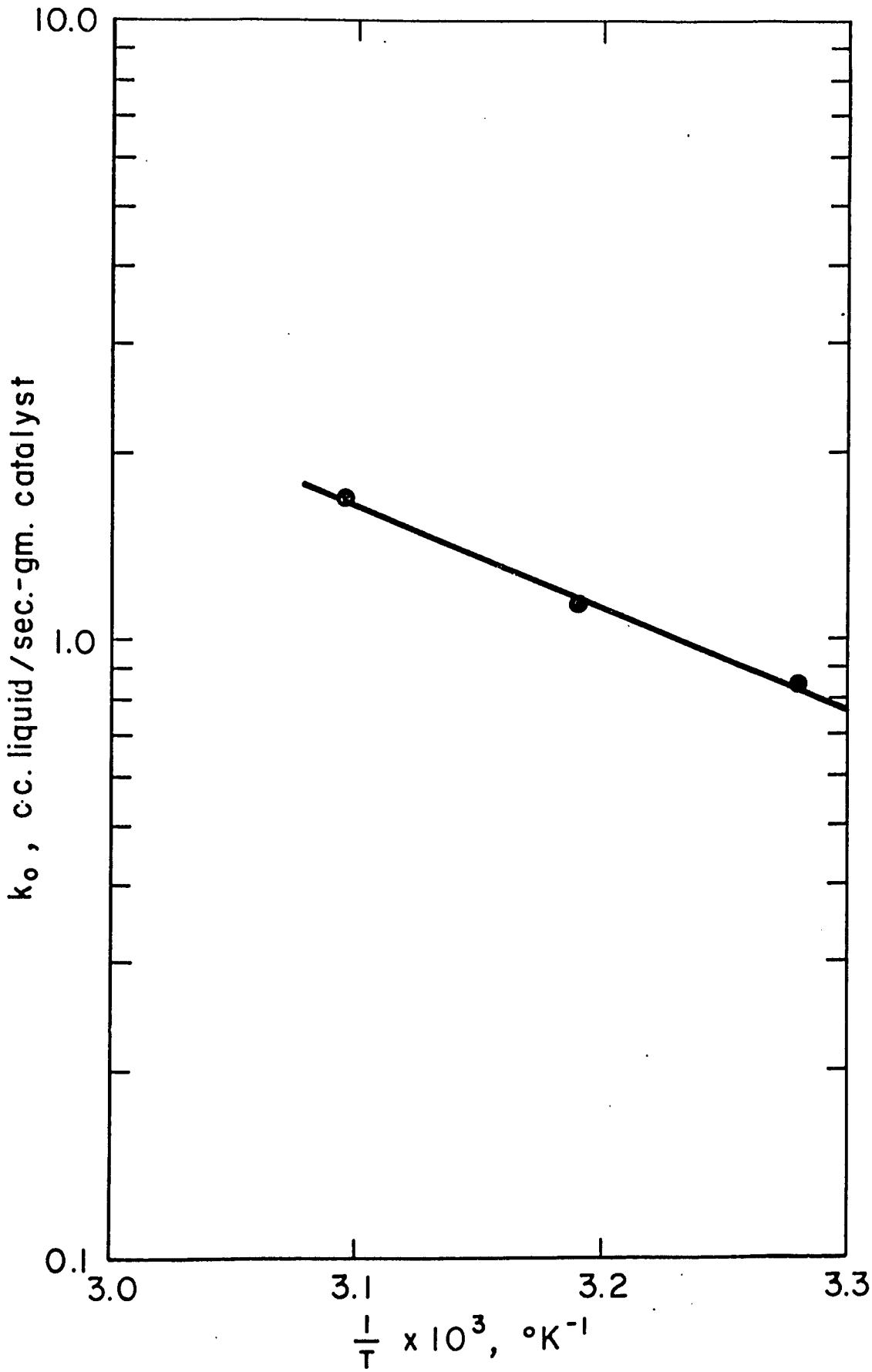

Figure III-9. Arrhenius Plot of Intrinsic Rate Constant versus the Reciprocal of Absolute Temperature

Reproduced with permission of the copyright owner. Further reproduction prohibited without permission.

little catalyst poisoning would have occurred (see, for example, Figure III-10 which is a plot of weight percent cumene in the effluent as a function of time for a typical run, Run 10). The results of Run 38 and Run 39 are compared in Figure III-11 with the results of Runs 7, 9, and 40 which were made with 100 grams of catalyst. All five runs were conducted at 32° C and liquid and gas flow rates of 100 cc/minute and 1 liter/minute respectively. Within the limits of the experimental error, a linear relationship exists between the rate of cumene formation and the catalyst weight. Indirectly, therefore, the conclusion can be drawn that the catalyst dilution ratio (within the range 0.0714 to 0.286 grams of catalyst per total bed weight) does not affect the reaction rate.

Near-isothermal conditions were met by the use of a diluted catalyst bed. The average temperature rise through the bed was approximately 1.0° C per one percent conversion at the lowest flow rates employed. At higher flow rates the temperature increase was slightly less than 1.0° C per one percent conversion. Similarly, radial temperature gradients were small. In one preliminary experiment the difference between the centerline and wall temperatures was

Reproduced with permission of the copyright owner. Further reproduction prohibited without permission.

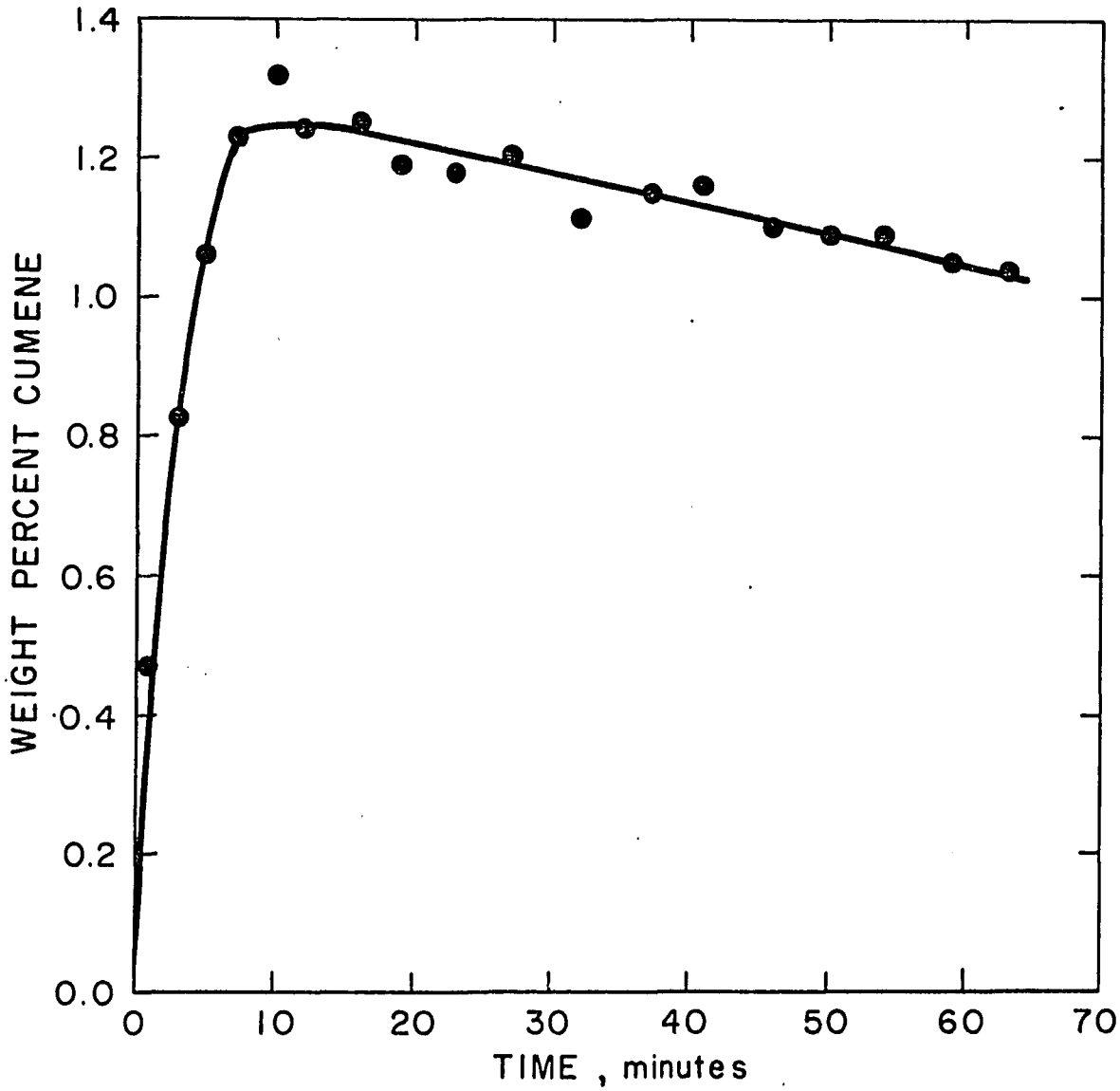

Figure III-10. Weight Percent Cumene in the Reactor Effluent as a Function of Time for Run 10

Reproduced with permission of the copyright owner. Further reproduction prohibited without permission.

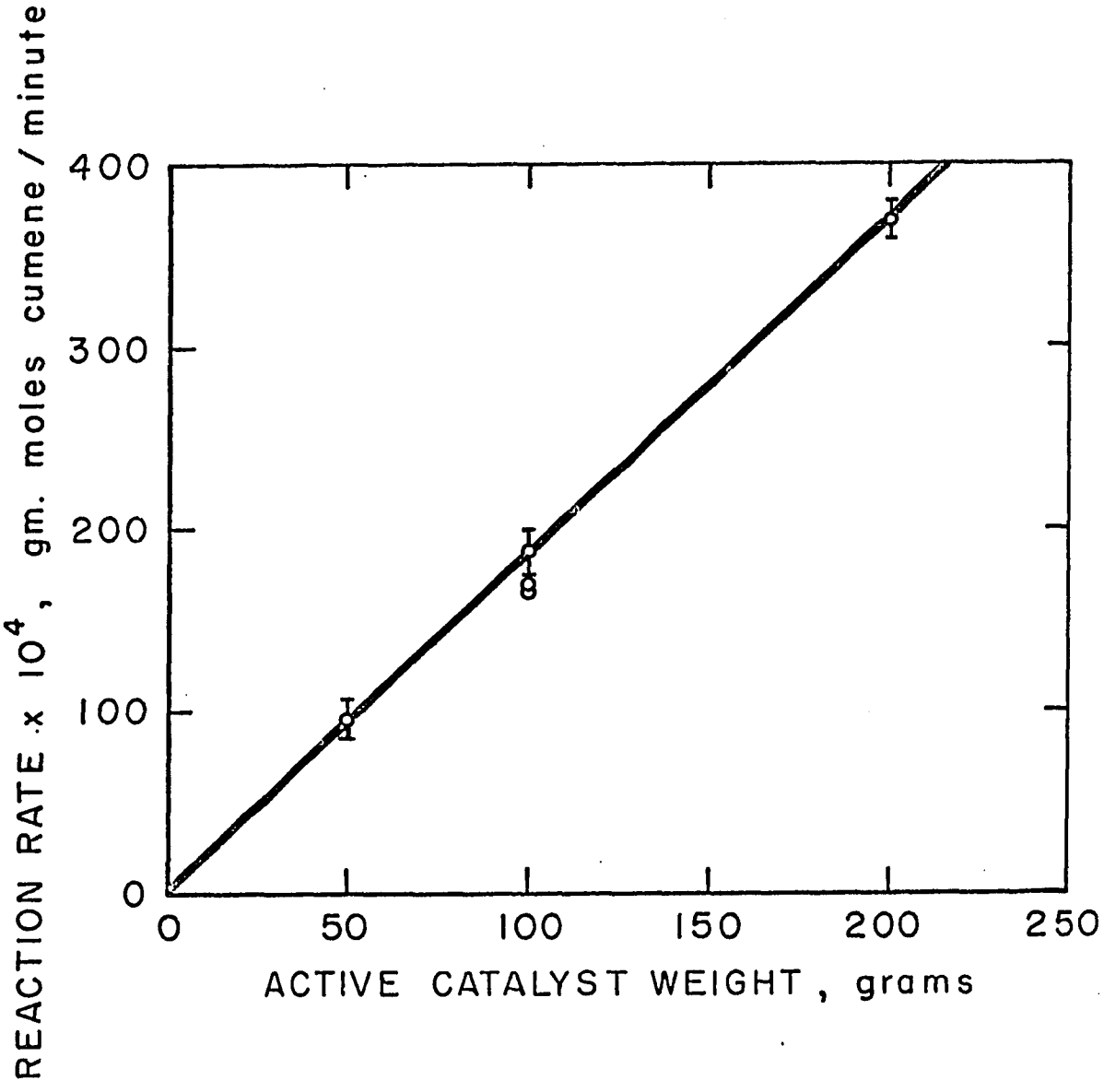

Figure III-11. Reaction Rate as a Function of Active Catalyst Weight for Five Runs at 32° C

Reproduced with permission of the copyright owner. Further reproduction prohibited without permission.

found to be about 1.0° C. This observation suggests that the liquid passing through the bed was evenly distributed in the radial direction and was of sufficient velocity to convectively remove much of the heat of reaction.

Reproduced with permission of the copyright owner. Further reproduction prohibited without permission.

CHAPTER IV

DISCUSSION OF RESULTS

There are two objectives of this chapter: the first goal is to develop the proposed mathematical model in detail including a justification of the assumptions of the model, and the second aim is to discuss the interpretation of the data in terms of the model.

A. Development of the Model

A comprehensive model to predict the rate of hydrogenation of alpha-methylstyrene to cumene in a trickle-bed reactor has to account for both individual catalyst pellet kinetics and the hydrodynamics of the flowing phases in the bed.

1. Fluid Hydrodynamics

At this point it would probably be helpful to summarize the literature results presented in Chapter I. While many types of mathematical models have been employed to characterize the axial mixing effects in packed beds, the results of experimental studies generally suggest that the degree of dispersion in the gas phase is small at low Reynolds numbers. The extent of liquid phase dispersion is

Reproduced with permission of the copyright owner. Further reproduction prohibited without permission.

greater than that of the gas phase, but a majority of the data on this topic has been obtained on Raschig rings in very long beds (five to twelve feet) where additional problems such as severe channeling and packing faults complicate the picture. Studies made on shorter beds indicate a closer approach to plug flow in the liquid phase. Radial velocity variations of both phases are generally negligible when the ratio of tube diameter to pellet diameter is greater than about thirty.

The packed bed used in the present investigation was 4.5 inches deep. The bed length to pellet diameter ratio was about 71/1 and the tube diameter to pellet diameter ratio was about 47/1. At the flow rates employed, the findings of other researchers summarized in the previous paragraph indicate that a simple liquid phase plug flow model may adequately describe the liquid hydrodynamics. Visual observations at start-up of the liquid flow through the glass-walled reactor support this suggestion. The spray-head distributor was highly efficient in wetting the entire top surface of the packing with small liquid drops. The gas phase is essentially all hydrogen and is present in the reactor in great excess relative to the amount of hydrogen consumed in the reaction. Since no homogeneous gas phase reaction occurs, it is not necessary to specify the flow

Reproduced with permission of the copyright owner. Further reproduction prohibited without permission.

profile or the extent of mixing in the gas phase. The only requirement is that the gas flow fast enough to continuously supply hydrogen to the catalyst as quickly as the chemical reaction consumes it. That is, the gas flow rate must be large enough to minimize external diffusion resistance.

Consider a differential element of the liquid phase in a trickle-bed reactor. For a reaction of the form $A_{(l)} + H_{2(g)} \longrightarrow D_{(l)}$ a steady-state material balance on product D yields,

$$r_D \, dW = F \, dX_D$$

Integrating over the reactor length,

$$W = \int_{X_{D_o}}^{X_{D_f}} \frac{F}{r_D} \, dX_D$$

For a zero order reaction in D, r_D is independent of X_D and

$$W = \frac{F \, \Delta X_D}{r_D} \quad \text{or} \quad r_D = \frac{F \, \Delta X_D}{W} \qquad \text{(IV-1)}$$

Equation (IV-1) relates the overall reaction rate to the overall conversion in a trickle-bed reactor. Since the reaction actually occurs at the catalyst surface, the rate of production of cumene, r_D, must be related to the surface concentrations of the reacting species. For a reaction of the form $A_{(l)} + H_{2(g)} \longrightarrow D_{(l)}$, the reaction rates are

Reproduced with permission of the copyright owner. Further reproduction prohibited without permission.

related by,

$$-r_A = -r_{H_2} = r_D$$

That is, the rate of production of D (cumene) is equal to the rate of depletion of H_2 (hydrogen). The individual catalyst pellet kinetics must now be established.

2. Individual Pellet Kinetics

The rate-controlling mechanism in a trickle-bed reactor can be one of or a combination of several steps, both physical and kinetic in nature. The following section is a discussion of all of these potential rate-limiting steps.

Physical Steps. There are four physical processes which may contribute to the overall reaction rate in a trickle-bed:

1. resistance to mass transfer in the gas phase,
2. mass transfer of reactants or products between the gas phase and the gas-liquid interface,
3. mass transfer through the liquid film surrounding the pellet,
4. diffusion of reactants or products within the catalyst pores.

Since the catalyst used in the present study was non-porous, step 4 was eliminated from consideration.

There was negligible resistance to transfer in the

Reproduced with permission of the copyright owner. Further reproduction prohibited without permission.

gas phase since it consisted almost entirely of hydrogen. The vapor pressures of alpha-methylstyrene and cumene do not exceed 15 mm. Hg. at 50° C, the highest temperature employed.

Step 2 is actually a study of the rate of absorption of hydrogen by alpha-methylstyrene since both alpha-methylstyrene and cumene have very low vapor pressures and thus remain in the liquid phase. Liquid film capacity coefficients at the gas-liquid interface have been correlated successfully (35, 42, 56, 57) by an equation of the form,

$$\frac{k_L a}{D} = \beta \left(\frac{L}{\mu}\right)^P \left(\frac{\mu}{\rho D}\right)^{0.5} \qquad \text{(IV-2)}$$

where the value of P is reported between 0.5 and 0.8. A similar correlation for the mass transfer coefficient is given by Shulman et al. (58). Other investigators (35, 45, 46) have simplified the equation to,

$$k_L a = HL^q \qquad \text{(IV-3)}$$

since at a fixed temperature parameters other than L are constant. In this equation, H and q are empirical constants, with q-values ranging from 0.6 to 0.9 depending upon the packing size. Although the forms of these correlations are slightly different, they both predict that the capacity coefficient increases with increasing liquid flow rate at a fixed temperature. This dependence can be qualitatively

Reproduced with permission of the copyright owner. Further reproduction prohibited without permission.

explained by the fact that turbulence produced by increased flow improves the mixing on the catalyst and hence increases the mass transfer rate. In the present study the experimental rate constant was not a function of the liquid (or gas) flow rate (Figures III-7 and III-8). Therefore, absorption mass transfer was not rate-controlling.

By a similar argument it can be shown that mass transfer through the liquid film surrounding the catalyst pellet is not the rate-limiting step. The molar mass flux of a component across the liquid film is the product of the diffusivity and the concentration gradient, i.e., $N = -D \frac{dC}{dZ}$. Since the alpha-methylstyrene is present at much higher concentrations than the hydrogen, the rate of diffusion of hydrogen through the film becomes rate-limiting before that of alpha-methylstyrene. Ma (40) has shown that the intrinsic kinetics are independent of the cumene concentration. Therefore, the diffusion of cumene through the liquid film could not affect the observed rate of reaction. Another potential resistance to mass transfer is the liquid film at the liquid-solid interface. Mass transfer rates through this film can be determined by studying the rates of dissolution of solids into liquids at very low liquid flow rates. These studies have already been made (68, 76, 77). van Krevelen and Krekels (68) investigated both liquid-continuous

Reproduced with permission of the copyright owner. Further reproduction prohibited without permission.

flow and film-like flow of several systems. Their results for film-like flow at Reynolds numbers between 10^{-2} and 20 were well correlated by,

$$Sh = 1.8\ Re^{1/2}\ Sc^{1/3} \qquad \text{(IV-4)}$$

where $Sh = \frac{k_L}{aD}$, $Re = \frac{U_L \rho}{a\mu}$, and $Sc = \frac{\mu}{\rho D}$. More recent analyses by Williamson et al. (76) and Wilson and Geankoplis (77) use the J-factor correlation,

$$J^{\varepsilon} = 1.09 \left(N_{Re}\right)^{-2/3} \qquad \text{(IV-5)}$$

where $J = \left(\frac{k_L}{U_L}\right)\left(\frac{\mu}{\rho D}\right)^{2/3}$.

This equation applies at Reynolds numbers between 10^{-3} and 55. Both of these correlations suggest that the mass transfer rate through the liquid film at the solid-liquid interface should increase with increasing liquid flow rate. Therefore, this mass transfer resistance was not significant in the present investigation.

In practice the rate of mass transfer across the entire liquid phase surrounding the solid pellet is determined by the rates across the films at the two interfaces plus the transfer rate through the bulk liquid. In trickle-flow operations the total film thickness is so small (typically 0.1 millimeter or less) that one can assume the

Reproduced with permission of the copyright owner. Further reproduction prohibited without permission.

bulk liquid layer is non-existent. The overall mass transfer coefficient, K_o, would then be expressed by an additive combination of the two film coefficients. That is,

$$\frac{1}{K_o} = \frac{1}{k_{L_1}} + \frac{1}{k_{L_2}} \qquad \text{(IV-6)}$$

where k_{L_1} and k_{L_2} are the mass transfer coefficients through the gas-liquid film and the liquid-solid film respectively. A two film analysis of this type has been employed successfully by Klassen and Kirk (35) and by Pelossof (47, 52). Obviously the overall coefficient, K_o, also increases with liquid flow rate. On this basis, therefore, the conclusion is reached that no mass transfer limitations existed in the trickle-bed reactor used in the present investigation.

Other evidence supports this conclusion. The effect of temperature on mass transfer coefficients is generally small. Look, for example, at the correlation of van Krevelen and Krekels (68), Equation (IV-7).

$$\frac{k_L}{aD} = 1.8 \left(\frac{U_L \rho}{a\mu} \right)^{1/2} \left(\frac{\mu}{\rho D} \right)^{1/3} \qquad \text{(IV-7)}$$

This correlation would predict a 16% increase in k_L on raising the temperature from 32° C to 50° C. Similarly, Equation (IV-2) would predict a 28% increase. Experimentally, the observed rate constant doubles over the

Reproduced with permission of the copyright owner. Further reproduction prohibited without permission.

same temperature range (see Tables III-1 and III-3). In addition, the reaction rate (gm. moles cumene/sec.) is linearly dependent on the catalyst weight (Figure III-11), a condition which would not be true if mass transfer were rate-controlling (3). Finally, the magnitude of the observed activation energy (7,280 cal./gm. mole) is typical of a chemical reaction controlled system. Activation energies for bulk diffusion (mass transfer control) are normally about 2 to 4 kcal/gm. mole.

Chemical Kinetic Steps. Two types of chemical steps could contribute to the overall reaction kinetics. These are:

1. adsorption or desorption of reactants or products on the catalyst surface,
2. intrinsic kinetics of reaction at the catalyst surface.

The adsorption isotherm theory as applied to surface kinetics (32) has probably received more attention in the literature than any other type of heterogeneous kinetic theory. Its good reputation has been earned by repeated successes in the field of heterogeneous catalysis. For this reason the adsorption isotherm theory is applied in the following analysis to determine the proper rate equation form.

Reproduced with permission of the copyright owner. Further reproduction prohibited without permission.

Before the theoretical analysis is begun, it is advantageous to review some of the kinetic literature on the hydrogenation of alpha-methylstyrene to form cumene. Ma (40) studied the reaction in a stirred tank with powdered palladium catalyst and found the intrinsic reaction rate was first order in hydrogen and independent of the concentration of cumene. Similar behavior has been reported with palladium black catalyst (20, 55) and with palladium-on-alumina catalyst (34, 47, 52). However, contrary to the findings of the other authors, Ma found that the reaction rate was also a function of the concentration of alpha-methylstyrene. His rate equation was,

$$r = \frac{k\, C_A\, P_{H_2}}{A + BC_A} \qquad \text{(IV-8)}$$

where k = reaction rate constant and A, B = constants which are functions of temperature only. Ma admits that the dependence on alpha-methylstyrene is not well established since its mole fraction was only varied between 0.8 and 1.0. Equation (IV-8) was empirically developed and, although Ma states that neither reactant is strongly adsorbed, his rate equation is of the form of a reaction which is influenced by alpha-methylstyrene adsorption. Indeed, in many hydrogenation reactions involving olefins or aromatics, the reactant molecule is usually strongly adsorbed (6, 10, 22,

Reproduced with permission of the copyright owner. Further reproduction prohibited without permission.

53, 59 p. 183, 60, 70). It would appear, therefore, that Ma's results may be equally well represented by a pseudo first order reaction in hydrogen. Babcock et al. (6) used palladium-on-alumina catalyst but reported a rate equation of a different form at hydrogen pressures above 3 atmospheres. The proposed form was,

$$r = k_s K_2 K_1 P_{H_2} X_\alpha \left[\frac{1}{1+ (K_2 P_{H_2})^{1/2}}\right]^2 \left[\frac{1}{1+ K_1 X_\alpha}\right] \qquad \text{(IV-9)}$$

However, Pelossof (47) has recently shown that Babcock's analysis is questionable. A recalculation of the catalyst effectiveness factor indicates that mass transfer resistance inside the catalyst pores was significant. The actual effectiveness factor was about 4% as compared with the value of 80 to 99% reported by Babcock. In summary, the intrinsic reaction rate of the hydrogenation of alpha-methylstyrene is first order in hydrogen concentration. Most investigators report no cumene or alpha-methylstyrene dependence. However, two studies do show a weak dependence of the reaction rate on the concentration of alpha-methylstyrene.

The most likely kinetic model for the present system involves a reaction between adsorbed alpha-methylstyrene and adsorbed atomic hydrogen in which the adsorption sites are adjacent. Recent data by Aben (1) on the palladium-

Reproduced with permission of the copyright owner. Further reproduction prohibited without permission.

hydrogen system substantiate the claim that hydrogen is atomically adsorbed (chemisorbed). The proposed adsorption model could be explained by a four step reaction sequence.

$$A + L \underset{k_1'}{\overset{k_1}{\rightleftharpoons}} AL \qquad K_1 = \frac{k_1}{k_1'} \qquad \text{(IV-10)}$$

$$H_2 + 2L \underset{k_2'}{\overset{k_2}{\rightleftharpoons}} 2HL \qquad K_2 = \frac{k_2}{k_2'} \qquad \text{(IV-11)}$$

$$AL + 2HL \underset{k_R'}{\overset{k_R}{\rightleftharpoons}} DL + 2L \qquad K_R = \frac{k_R}{k_R'} \qquad \text{(IV-12)}$$

$$DL \underset{k_3'}{\overset{k_3}{\rightleftharpoons}} D + L \qquad K_3 = \frac{k_3}{k_3'} \qquad \text{(IV-13)}$$

In Equations (IV-10) through (IV-13) the following symbols are used:

A = alpha-methylstyrene molecule

H_2 = hydrogen molecule

D = cumene molecule

L = vacant catalyst site

AL = adsorbed alpha-methylstyrene molecule

HL = adsorbed hydrogen atom

DL = adsorbed cumene molecule

K_1, K_2 = adsorption equilibrium constants for alpha-methylstyrene and hydrogen respectively

Reproduced with permission of the copyright owner. Further reproduction prohibited without permission.

K_3 = desorption equilibrium constant for cumene

K_R = reaction equilibrium constant

k, k' = forward and reverse rate constants

In addition to these four equations, an equation for the number of catalyst sites is needed (Equation IV-14).

$$L_T = C_L + C_P + C_{AL} + C_{HL} + C_{DL} \qquad \text{(IV-14)}$$

In Equation (IV-14),

L_T = total number of sites

C_L = number of vacant active sites

C_P = number of "poisoned" active sites

C_{AL}, C_{HL}, C_{DL} = number of sites occupied by alpha-methylstyrene, hydrogen, and cumene respectively.

If the adsorption of alpha-methylstyrene is the rate-controlling step, the reaction rate is given by,

$$r = k_1 C_A C_L - k_1' C_{AL} \qquad \text{(IV-15)}$$

Reactions (IV-11), (IV-12), and (IV-13) are assumed to be at equilibrium. Therefore,

$$k_2 C_{H_2} C_L^2 = k_2' C_{HL}^2 \qquad \text{(IV-16)}$$

$$k_R C_{AL} C_{HL}^2 = k_R' C_{DL} C_L^2 \qquad \text{(IV-17)}$$

$$k_3 C_{DL} = k_3' C_D C_L \qquad \text{(IV-18)}$$

Reproduced with permission of the copyright owner. Further reproduction prohibited without permission.

From Equations (IV-16) and (IV-18),

$$C_{HL}^2 = K_2 C_{H_2} C_L^2 \qquad \text{(IV-19)}$$

$$C_{DL} = \frac{C_D C_L}{K_3} \qquad \text{(IV-20)}$$

Substitution of Equations (IV-19) and (IV-20) into (IV-17) gives,

$$C_{AL} = \frac{C_D C_L}{K_2 K_3 K_R C_{H_2}} \qquad \text{(IV-21)}$$

Equation (IV-14) can be expressed as,

$$C_L = (L_T - C_P) - C_{AL} - C_{HL} - C_{DL} \qquad \text{(IV-22)}$$

Substituting Equations (IV-19), (IV-20), and (IV-21) into Equation (IV-22), and collecting terms gives,

$$C_L = \frac{(L_T - C_P)}{\left[1 + \frac{C_D}{K_2 K_3 K_R C_{H_2}} + (K_2 C_{H_2})^{1/2} + \frac{C_D}{K_3}\right]} \qquad \text{(IV-23)}$$

Substituting Equations (IV-21) and (IV-23) into Equation (IV-15) yields,

$$r = \frac{k_1 (L_T - C_P)}{K_1} \left[\frac{K_1 C_A - \frac{C_D}{K_2 K_3 K_R C_{H_2}}}{1 + \frac{C_D}{K_2 K_3 K_R C_{H_2}} + (K_2 C_{H_2})^{1/2} + \frac{C_D}{K_3}}\right] \qquad \text{(IV-24)}$$

Reproduced with permission of the copyright owner. Further reproduction prohibited without permission.

The reaction rate is thus given by Equation (IV-24) in which C_A, C_{H_2}, and C_D represent the surface concentrations of alpha-methylstyrene, hydrogen, and cumene, respectively. The reaction equilibrium constant, K_R, can be calculated from thermodynamic data and is equal to about 10^{12} at 25° C. Therefore, the reverse reaction is negligible. The equation then becomes,

$$r = \frac{k_1 (L_T - C_P) C_A}{\left[1 + (K_2 C_{H_2})^{1/2} + \frac{C_D}{K_3}\right]} \qquad \text{(IV-25)}$$

Equation (IV-25) does not predict the first order hydrogen dependence and, therefore, adsorption of alpha-methylstyrene is not rate-controlling.

If desorption of cumene is the rate-limiting step, by a similar analysis the reaction rate is expressed by Equation (IV-26),

$$r = k_3 (L_T - C_P) \qquad \text{(IV-26)}$$

Again the incorrect hydrogen dependence is predicted and thus the rate of desorption of cumene is not rate-limiting.

If the rate of adsorption of atomic hydrogen is assumed to be rate-controlling, the reaction rate is,

$$r = \frac{k_2 (L_T - C_P)^2 C_{H_2}}{(1 + K_1 C_A + K_3' C_D)^2} \qquad \text{(IV-27)}$$

Reproduced with permission of the copyright owner. Further reproduction prohibited without permission.

where K_3' is the adsorption equilibrium constant for cumene. Generally, in the hydrogenation of hydrocarbons and aromatics, the adsorption of the hydrogenated product is small compared to the reactant adsorption (6, 59 p. 182). In addition, in the differential reactor employed in the present study, the cumene mole fraction was always less than 0.05: Thus the term $K_3' C_D$ in Equation (IV-27) can be neglected. On the other hand, the aromatic reactant molecule is usually strongly adsorbed in hydrogenation reactions (6, 10, 22, 53, 59 p. 183, 60, 70). Since the percentage of alpha-methylstyrene in the liquid phase was always greater than 95% in this investigation, the term $K_1 C_A$ in Equation (IV-27) is large and is probably much greater than unity. For instance, data analyzed by Sawyer and Mezaki (53) for the hydrogenation of a series of olefins indicate that the adsorption constant of the olefin increases with increasing molecular weight. The value for mixed iso-octenes is 3000 $atm.^{-1}$ whereas the adsorption constant for ethylene is 3.32 atm^{-1}. In all cases studied the olefin adsorption constant was at least two orders of magnitude greater than the hydrogen adsorption constant. Similarly, for the hydrogenation of alpha-methylstyrene reaction reported by Babcock and coworkers (6), the hydrogen adsorption constant

Reproduced with permission of the copyright owner. Further reproduction prohibited without permission.

was about 100 times smaller than that of alpha-methylstyrene. Therefore, Equation (IV-27) reduces to,

$$r = \frac{k_2 (L_T - C_P)^2 C_{H_2}}{(1 + K_1 C_A)^2} = k_2^* (L_T - C_P)^2 C_{H_2} \qquad \text{(IV-28)}$$

Equation (IV-28) indicates that the rate of reaction is pseudo first order in hydrogen, k_2^* being the pseudo first order rate constant.

If the surface reaction is rate-controlling, the reaction rate is expressed by Equation (IV-29).

$$r = \frac{k_R (L_T - C_P)^3 K_1 K_2 C_A C_{H_2}}{(1 + K_1 C_A + (K_2 C_{H_2})^{1/2} + K_3' C_D)^3} \qquad \text{(IV-29)}$$

Employing the same arguments as given in the previous paragraph, the last two terms in the denominator can be neglected. If $K_1 C_A \gg 1$, the equation becomes,

$$r = \frac{k_R (L_T - C_P)^3 K_2 C_{H_2}}{(1 + K_1 C_A)^2} = k_R^* (L_T - C_P)^3 C_{H_2} \qquad \text{(IV-30)}$$

which is of the same form as Equation (IV-28) except that k_R^* is now the pseudo first order rate constant. Thus, it is not possible to determine, from only the form of the rate equation, whether hydrogen adsorption or surface reaction

Reproduced with permission of the copyright owner. Further reproduction prohibited without permission.

is the rate-limiting step. Of course, it is possible that both steps are rate-controlling. An examination of the observed activation energy should shed some light on the apparent rate-limiting step. Heats of adsorption for hydrogen on metals of the platinum group are in general highly exothermic. Typical examples are platinum (10-30 kcal./gm. mole), nickel (10-30 kcal./gm. mole) and palladium (12-30 kcal./gm. mole). The intrinsic activation energy for the hydrogenation of alpha-methylstyrene on powdered palladium catalyst was reported by Ma (40) to be 7,600 cal./gm. mole. The activation energy experimentally determined in the present investigation was 7,280 $\pm$ 337 cal./gm. mole. It appears likely, therefore, that the surface reaction was the slowest step and the reaction rate is given by Equation (IV-30).

The term $(L_T - C_P)^3$ in Equation (IV-30) is the deactivation or poisoning function which is comparable to ϕ in Equation (III-2). While L_T is a constant for a given weight of catalyst, the number of poisoned sites, C_P, increases with time of usage of the catalyst. Therefore, the variable $(L_T - C_P)$ decreases with time, as does the function ϕ . The exponential dependence of the poisoning rate on time is similar to that observed by Weekman (71) and by Kunugita and coworkers (36). General poisoning

Reproduced with permission of the copyright owner. Further reproduction prohibited without permission.

functions, including exponential behavior, have been considered by other researchers (9, 62).

The total number of useful active catalyst sites, $(L_T - C_P)$, could be expected to be a linear function of the catalyst weight. Therefore, the reaction rate as predicted by Equation (IV-30) should be a function of the cube of the catalyst weight. However, the data of the present study suggest that this is not true (see, for example, Figure III-11). This lack of agreement between the predictions of the adsorption isotherm theory and the experimental data is probably a result of an assumption made in the theory which is not entirely correct. This theory assumes that each catalyst site has equal activity. In reality, however, it is known that some sites are more active than others and so the surface atoms have a distribution of activities or energies. Since little is known regarding the form of this distribution, consider for illustrative purposes a normal distribution of site activities. According to this distribution, a small number of the sites would be highly active and a small fraction would be relatively inactive. The majority of the sites would possess some activity between these two extremes. If one accepts the assumption that the most active sites would be poisoned first, then as the poisoning continues both the total number of unpoisoned sites and the

Reproduced with permission of the copyright owner. Further reproduction prohibited without permission.

activity of the average site would decrease with time. It would thus be very difficult to predict the exact functional relationship between the reaction rate on a poisoned catalyst and the time. An empirical approach (such as the one employed here) to the prediction of the deactivation rate is usually necessary. Therefore, due to the distribution of catalyst site activities, the adsorption isotherm theory of catalysis would not be expected to predict the correct form of the deactivation function. In order to do this a theory would have to take into account not only the number of unpoisoned sites but also the activity distribution of the sites. While the adsorption isotherm theory fails to predict the proper deactivation rate, it has been very successful in many applications in predicting the correct concentration dependence of the reaction rate. This is presumably because the combination of reactant molecules on the catalyst surface can occur on sites of a wide range of activities whereas catalyst poisoning is a very specific process which probably starts on the most active sites and in time proceeds towards the least active ones.

In summation, the rate-controlling step in the hydrogenation of alpha-methylstyrene in a trickle-bed reactor is most likely a surface reaction between weakly adsorbed hydrogen atoms and strongly adsorbed alpha-methylstyrene

Reproduced with permission of the copyright owner. Further reproduction prohibited without permission.

molecules. The form of the rate equation can be explained by the adsorption isotherm theory and is in agreement with rate equations for similar systems presented by other investigators. The proposed equation is,

$$r_D = \frac{F\ \Delta X_D}{W} = k_o\ \phi\ C^*$$

where $\phi = e^{-\alpha\tau}$ and $k_o = k_o'\ e^{-E_a/RT}$. (IV-31)

B. Interpretation of Results

The proposed rate equation indicates a first order or pseudo first order hydrogen dependence coupled with a temperature dependent rate constant and a deactivation function which is time dependent.

There is considerable evidence that external mass transfer did not play a limiting role in this investigation. Within the limits of error of the rate constant, the gas and liquid flow rates had no effect on k_o (Figures III-5 through III-8). The reaction rate increased linearly with catalyst weight over the range from 50 grams to 200 grams (Figure III-11). If diffusion limitations existed, the curve in Figure III-11 would have risen at a slower rate at the higher catalyst loadings than at the lower ones, due to the inability of hydrogen to diffuse to the catalyst surface

Reproduced with permission of the copyright owner. Further reproduction prohibited without permission.

fast enough to supply the reaction. Final proof of reaction control is the large effect of temperature on the observed rate. A doubling of the rate constant over a temperature range of 18° C is far greater than the effect predicted by any mass transfer theory. An estimated film thickness of only 0.1 mm. certainly suggests that mass transfer limitations are small.

It was established that the unpoisoned catalysts yielded reasonably repeatable reaction rates and rate constants from one batch to the next. The average standard deviation of the rate constants was about 10% (see Tables III-1, III-2, and III-3). On Figure III-11 the three points at 100 grams loading represent reaction rates measured on three different batches of fresh catalyst. The points differ by about 10%. Therefore fresh catalyst activity varied by no more than the activity of a single loading of catalyst.

The magnitude of the calculated activation energy is in excellent agreement with the value determined by Ma (40) for the intrinsic reaction carried out over powdered palladium catalyst. Ma's activation energy was 7,600 cal./gm.mole as compared with the presently observed value 7,280 $\pm$ 337 cal./gm. mole. The activation energy determined by Pelossof (47) in a pore-diffusion limited system was

Reproduced with permission of the copyright owner. Further reproduction prohibited without permission.

5,080 ± 500 cal./gm. mole which is consistent with the value of the activation energy for the intrinsic reaction.

The reaction rate constants ranged from 0.841 ± 0.073 to 1.69 ± 0.17 cc. liq./sec.-gm. cat. The unusual units associated with k_o are, of course, a result of the form of the rate equation. Ideally, for a first order reaction, the rate constant has inverse time units. For comparison purposes one could adjust the observed rate constants to units of inverse seconds by multiplying by the catalyst weight (100 grams) and by estimating the liquid held-up on the catalyst. For example, assuming that 40% of the bed voids are filled by liquid (50), the adjusted rate constants would range from 5.30 $sec.^{-1}$ at 32° C to 10.7 $sec.^{-1}$ at 50° C. This latter value is in reasonable agreement with the intrinsic rate constant reported by Ma (40) of 16.8 $sec.^{-1}$ at 50° C. The excellent correspondence between the rate constants and activation energies reported in this thesis and by Ma (40) and Pelossof (47) could be expected since both catalysts were prepared by depositing a palladium salt on a support with subsequent reduction. The fact that Ma reports weak adsorption of alpha-methylstyrene is not too surprising since adsorption constants are usually highly dependent on temperature. Therefore, in contrast to the strong adsorption observed by some investigators (6) at

Reproduced with permission of the copyright owner. Further reproduction prohibited without permission.

30° C, the adsorption may have indeed been weak in the 70° C to 100° C range studied by Ma. The rate constant on palladium black as determined by Farkas (20) was slightly lower, about 1.0 sec^{-1}. However, since Farkas was not able to completely exclude diffusion effects, his rate constant should be lower than the intrinsic value.

While isothermal conditions were not precisely attained in this study, temperature gradients were small. As mentioned in Chapter III, radial temperatures differed by about 1.0° C between the wall and the center-line and axial gradients amounted to about a 1.0° C temperature rise for each one percent of conversion. For the same reaction Babcock and coworkers (6) measured approximately a 3.0° C temperature increase per one percent conversion in a differential bed reactor. Therefore, at a maximum of three percent conversion, their total temperature rise was about 9.0° C across a three centimeter long bed. At 25° C this represents an error in temperature of 36% which leads one to question the preciseness of their data. Although truly isothermal conditions did not exist in the reactor employed in the present investigation, the diluted catalyst reactor apparently does offer better temperature control than the equivalent differential trickle-bed reactor.

The poisoning of the palladium surface by traces of

Reproduced with permission of the copyright owner. Further reproduction prohibited without permission.

copper atoms created some problems in analyzing the kinetic data. In order to correct for the deactivation, it was necessary to extrapolate the rate data to zero time. Fortunately, because of the frequency of measurements taken in this study, the extrapolation was over a short time period (30 to 60 minutes). The small temperature effect on the slopes of the curves in Figures III-1, III-2, and III-3 may be a result of increased copper concentrations in the alpha-methylstyrene accompanying a rise in temperature. Although the change in slope could also be simply a result of experimental error, this possibility is lessened by the close agreement between the slope of the Run 40 data and the slope of the remaining 32^{o} C data. At first it was thought that the poison was polymer being formed on and remaining on the catalyst surface. Viscosity measurements of the liquid feed and product solutions detected no polymers. No polymers precipitated from the solutions when large volumes of methanol were added to the liquid feed and product samples. In addition, the slope of the deactivation curves, α , increases approximately exponentially with temperature. The activation energy associated with α is about 3 kcal/gm mole. The activation energy for the thermal polymerization of styrene is 29 kcal/gm. mole (21), which again suggests that adsorbed polymers were not the cause of the

Reproduced with permission of the copyright owner. Further reproduction prohibited without permission.

deactivation. The negligible effect of the change in start-up procedures suggests that the poisoning was not related to the formation of oxidation products or similar poisons between runs. Nor was the deactivation a result of abrasive removal of the palladium from the catalyst surface. One disadvantage of non-porous catalysts is that they do tend to adsorb poisons and deactivate (75, p. 277). This is due to the fact that the surface area is so small that, when poisoning does occur, the rate of deactivation can be significant. Maxted (41), in a survey of catalysts poisoned by toxic metals, found that many metal poisons inhibit the activity of platinum and palladium. The only metal of any consequence used in the equipment was copper in the form of a 30 foot heating coil. An analysis for metal poisons on the catalyst was made on a Jarrell-Ash Optical Emission Spectrograph. The only metal detected on the used catalyst (total time of usage about 2 hours) that was not found on fresh catalyst or dolomite samples was copper. The concentration was estimated between 10 and 100 parts of copper per million parts of all elements. However, since dolomite is a non-porous mineral, the copper surface concentration was probably several times the reported value. One can

Reproduced with permission of the copyright owner. Further reproduction prohibited without permission.

thus conclude that the catalyst poison was copper. The copper was removed from the copper tubing by alpha-methylstyrene and was strongly adsorbed by the catalyst as the liquid passed through the bed. The adsorption of the copper apparently resulted in continuing catalyst deactivation with time.

Reproduced with permission of the copyright owner. Further reproduction prohibited without permission.

CHAPTER V

CONCLUSIONS AND RECOMMENDATIONS

A number of conclusions can be drawn from the information obtained in this investigation.

This work is the first reported study of the measurement of intrinsic reaction rates in a diluted catalyst trickle-bed reactor employing a non-porous catalyst. For a highly exothermic three phase reaction, namely the hydrogenation of alpha-methylstyrene, a reactor of this type permits the acquisition of near-isothermal intrinsic kinetic data on a supported catalyst. In all previous trickle-bed kinetic investigations, porous catalysts were used which had low effectiveness factors. Since the internal surface area available for reaction can not be precisely known, particularly in the case of liquid filled catalyst pores, a determination of the exact contribution of the internal pore conversion to the overall reactor conversion is difficult. Therefore, in a trickle-bed reactor, intrinsic reaction rate data should be more reliably obtained on a non-porous catalyst than on a porous one.

The data is described, within an accuracy of about 10%, by a kinetic model which assumes the liquid phase is

Reproduced with permission of the copyright owner. Further reproduction prohibited without permission.

in plug flow, the surface reaction rate is first order in hydrogen pressure, and the catalyst activity decreases exponentially with time. The calculated activation energy for the intrinsic reaction, 7,280 cal./gm. mole, agrees well with the value obtained by Ma (40) on a powdered palladium catalyst in a stirred tank reactor, 7,600 cal./gm. mole.

External diffusion resistances were reduced to a minimum in the trickle-bed reactor by proper choices of the gas and liquid flow rates and the bed temperature. For the hydrogenation of alpha-methylstyrene the reactor was effective at room conditions. At these temperatures external diffusion limitations were minimized and adverse side reactions such as polymerization did not occur.

In consideration of the findings of the present investigation, the following recommendations are made.

Although they have relatively low surface areas, nonporous catalysts may be industrially important for special applications. These catalysts should be superior to porous catalysts for reactions in which a long pore residence time cannot be tolerated. Examples are reactions of hydrocarbons in which unwanted polymerization or cracking of molecules may occur due to excessive residence times in contact with active catalyst. In accordance with these ideas, it may be

Reproduced with permission of the copyright owner. Further reproduction prohibited without permission.

of interest to compare the long term performances of porous and non-porous catalysts in promoting the hydrogenation of a monomer such as styrene to form ethylbenzene. The non-porous catalyst may prove to be just as effective as the porous catalyst because of pore blockage by polymer formed by a side reaction.

A survey of the literature shows that very little data exists on pressure drop and liquid holdup in cocurrent downflow trickle-columns packed with small irregular granules. A majority of the work has been done on Raschig rings and Berl saddles. New data and correlations which are applicable to irregular granules would be helpful to future researchers.

Reproduced with permission of the copyright owner. Further reproduction prohibited without permission.

APPENDIX A

CHROMATOGRAPHIC ANALYSIS

An F and M Model 700 Gas Chromatograph equipped with a thermal conductivity detector was employed to analyze the liquid samples. The column was 6 feet of Carbowax 20 M on 60-80 mesh Diatoport S support. Helium carrier gas at a flow rate of 50 cc/min. and 30 psi pressure optimized the separation of component peaks and permitted the analysis of a sample to be completed within three minutes. Injection port, oven, and detector temperatures were 190° C, 160° C, and 195° C, respectively, and the bridge current was 150 milliamperes. A ten microliter syringe was used to deliver a five microliter sample to the chromatograph.

The chromatograph was calibrated by making ten duplicate five microliter injections of each of alpha-methylstyrene, isopropylbenzene (cumene) and normal propyl benzene. An additional ten microliter sample of each component demonstrated the independence of chromatograph response on sample size. Although the normal propyl benzene did not participate in the chemical reaction, it was present as an impurity in the commercial alpha-methylstyrene at a concentration of about 0.55 weight

Reproduced with permission of the copyright owner. Further reproduction prohibited without permission.

percent. Therefore, it was necessary to calibrate the chromatograph for it. Analyses of the reactor feed and product solutions proved that this impurity was not involved in the reaction and that its concentration did not vary from run to run. The disc chart integrator on the Honeywell chromatograph recorder was used to measure the area under the component peaks. The ten areas for each component were averaged and then adjusted to an attenuation of 128. Choosing alpha-methylstyrene (AMS) as a standard, weight factors for isopropylbenzene (IPB) and n-propyl benzene (NPB) were calculated from

$$\text{IPB weight factor} = \frac{\text{average area of IPB peak}}{\text{average area of AMS peak}}$$

$$\text{NPB weight factor} = \frac{\text{average area of NPB peak}}{\text{average area of AMS peak}}$$

The results were

AMS weight factor = 1.00

IPB weight factor = 0.954

NPB weight factor = 0.957

This calibration method is permissible since the densities of all three components are very similar.

The weight factors were employed in the following way. The three areas for a single product sample were measured using the disc integrator. The areas for isopropylbenzene

Reproduced with permission of the copyright owner. Further reproduction prohibited without permission.

and n-propylbenzene were corrected by multiplying by their respective weight factors. The weight percent of each component is then given by,

$$\text{Weight percent IPB} = \frac{\text{Corrected area of IPB peak}}{\text{Total corrected areas of all three peaks}} \times 100$$

$$\text{Weight percent NPB} = \frac{\text{Corrected area of NPB peak}}{\text{Total corrected areas of all three peaks}} \times 100$$

$$\text{Weight percent AMS} = 100 - (\text{Wt \% IPB}) - (\text{Wt \% NPB}).$$

After it was conclusively demonstrated that the n-propyl benzene did not participate in the reaction and was present in a constant concentration, the analysis was modified as follows:

$$\text{Weight percent IPB} = \frac{\text{Corrected area of IPB peak}}{\text{Total corrected areas IPB and AMS peaks}} \times 100$$

$$\text{Weight percent AMS} = 100 - (\text{Weight percent IPB}).$$

Some of the samples could not be reliably analyzed due to a poor injection technique which resulted in severe tailing and overlap of the peaks. These samples are indicated in the data as poor injections.

The weight factors were rechecked near the conclusion of the experimental portion of the research and were found to be unchanged.

Reproduced with permission of the copyright owner. Further reproduction prohibited without permission.

APPENDIX B

OPERATING CONDITIONS AND CATALYST DATA

Table B-1. Data on Catalyst and Reactor Bed

Table B-2. Summary of Run Conditions

Reproduced with permission of the copyright owner. Further reproduction prohibited without permission.

TABLE B-1

DATA ON CATALYST AND REACTOR BED

Catalyst

1. 0.3 weight % palladium deposited on non-porous dolomite.
2. Irregular catalyst granules, average diameter 1.61 mm.
3. Pellet density, 2.86 grams/cc.
4. Catalyst surface area (calculated), 52.3 $cm.^2/gm.$

Reactor Bed

1. Bed volume, 521 cc.
2. Bed density, 1.34 grams/cc.
3. Void fraction, 0.532 cc. voids/cc. bed
4. Dilution ratio: (all runs except numbers 38 and 39), 100 grams catalyst/600 grams inert dolomite
5. Dilution ratio: (Run 38), 50 grams cat./650 grams dolomite

   (Run 39), 200 grams cat./500 grams dolomite

Method of Preparation

1. Dolomite particles are impregnated with $PdCl_2$ in HCl soln.
2. Then ph is adjusted to 6 with several room temperature washes with $NaHCO_3$. This gels the Pd solution into a Pd-oxide gel.
3. During foregoing gel, crystallites of Pd-oxide hydrate grow on the dolomite surface.
4. Catalyst is then thoroughly water washed to remove most if not all of the chloride ion.
5. Catalyst is then air dried.

Note:

The catalyst was manufactured by the Houdry Process and Chemical Company.

Reproduced with permission of the copyright owner. Further reproduction prohibited without permission.

TABLE B-2

SUMMARY OF RUN CONDITIONS

Run Number	Liquid Flow Rate, L, cc./min.	Gas Flow Rate, G, liters/min.	Temperature ^{0}C
7[a]	100	1.0	32
8	100	1.0	
9[a]	100	1.0	
10	100	1.0	
11	100	1.8	
12	100	2.5	
13	100	1.0	
14	100	1.0	
15	160	1.0	
16	160	1.8	
17	160	2.5	
18[a]	100	1.0	50
19	100	1.0	
20	100	1.0	
21	100	1.8	
22	160	1.8	
23	225	1.8	
24	100	2.5	
25	225	2.5	
26	160	2.5	
27	160	2.5	
28	160	2.5	
30[a]	160	1.0	40
31	100	1.0	
32	225	1.0	

Reproduced with permission of the copyright owner. Further reproduction prohibited without permission.

TABLE B-2--Continued

Run Number	Liquid Flow Rate, L, cc./min.	Gas Flow Rate, G, liters/min.	Temperature ^{0}C
33	225	2.5	40
34	160	2.5	
35	100	2.5	
36	225	1.8	
37	160	1.8	
38[b]	100	1.0	32
39[c]	100	1.0	
40[a]	100	1.0	

[a]Fresh catalyst, 100 grams cat./600 grams dolomite

[b]Fresh catalyst, 50 grams cat./650 grams dolomite

[c]Fresh catalyst, 200 grams cat./500 grams dolomite

Reproduced with permission of the copyright owner. Further reproduction prohibited without permission.

APPENDIX C

PHYSICAL PROPERTIES OF THE FLUIDS

Figure C-1. Densities of Alpha-methylstyrene and Cumene as Functions of Temperature

Figure C-2. Vapor Pressure of Alpha-methylstyrene as a Function of Temperature

Figure C-3. Viscosity of Alpha-methylstyrene as a Function of Temperature

Figure C-4. Diffusivity of Hydrogen in Alpha-methylstyrene as a Function of Temperature

Figure C-5. Solubility of Hydrogen in Alpha-methylstyrene as a Function of Temperature at One Atmosphere Pressure

Note:

The data on these figures was extracted with permission from Reference 47.

Reproduced with permission of the copyright owner. Further reproduction prohibited without permission.

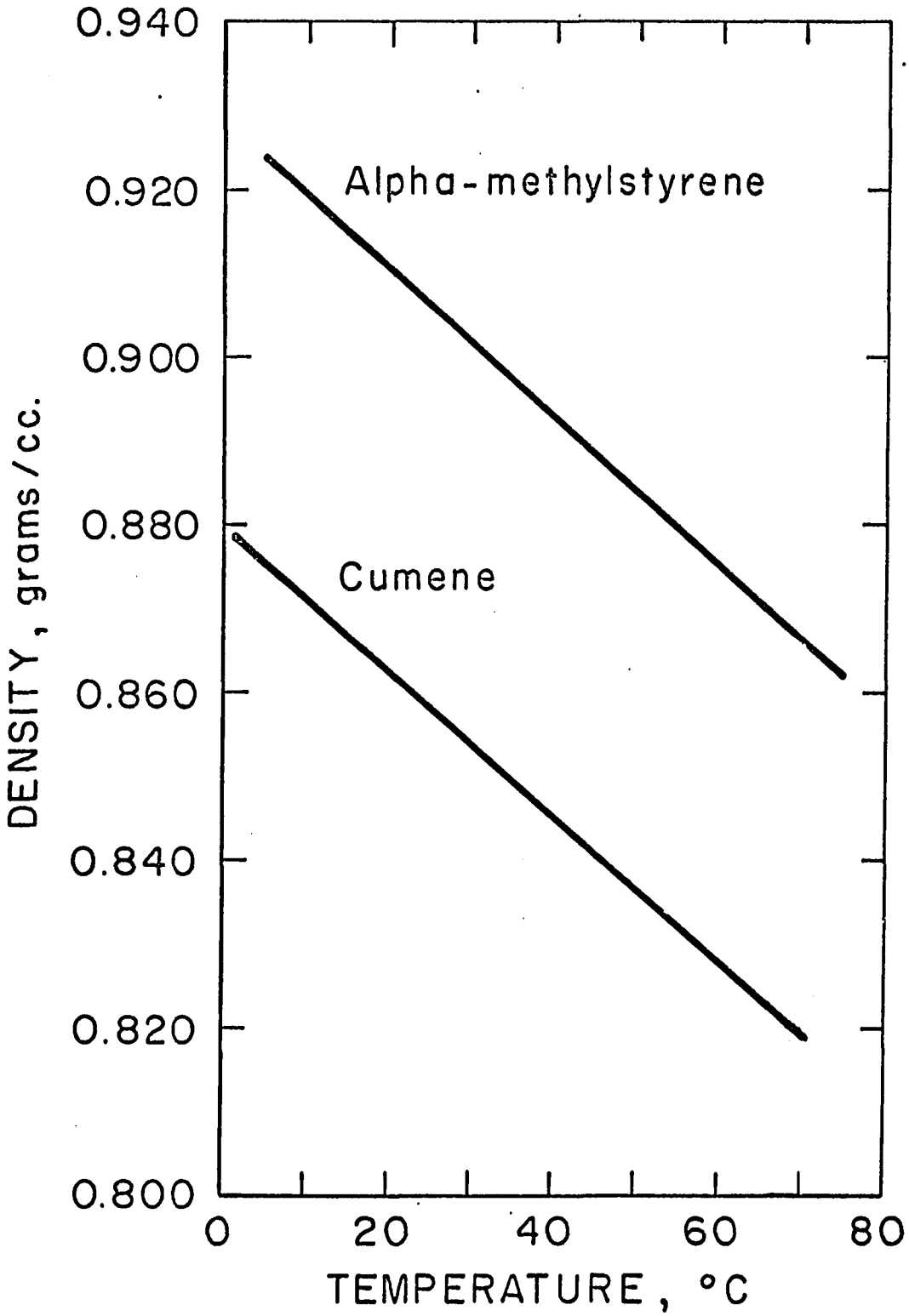

Figure C-1. Densities of Alpha-methylstyrene and Cumene as Functions of Temperature

Reproduced with permission of the copyright owner. Further reproduction prohibited without permission.

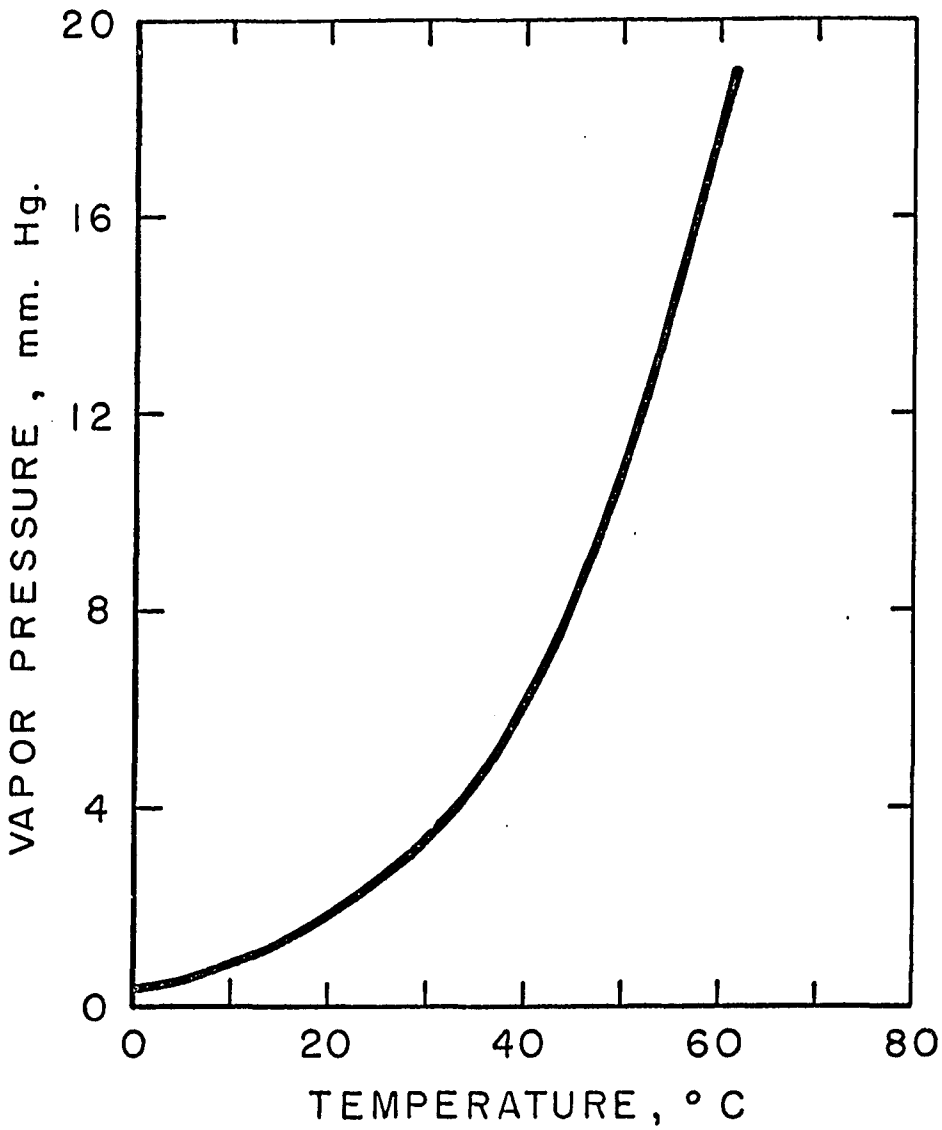

Figure C-2. Vapor Pressure of Alpha-methylstyrene as a Function of Temperature

Reproduced with permission of the copyright owner. Further reproduction prohibited without permission.

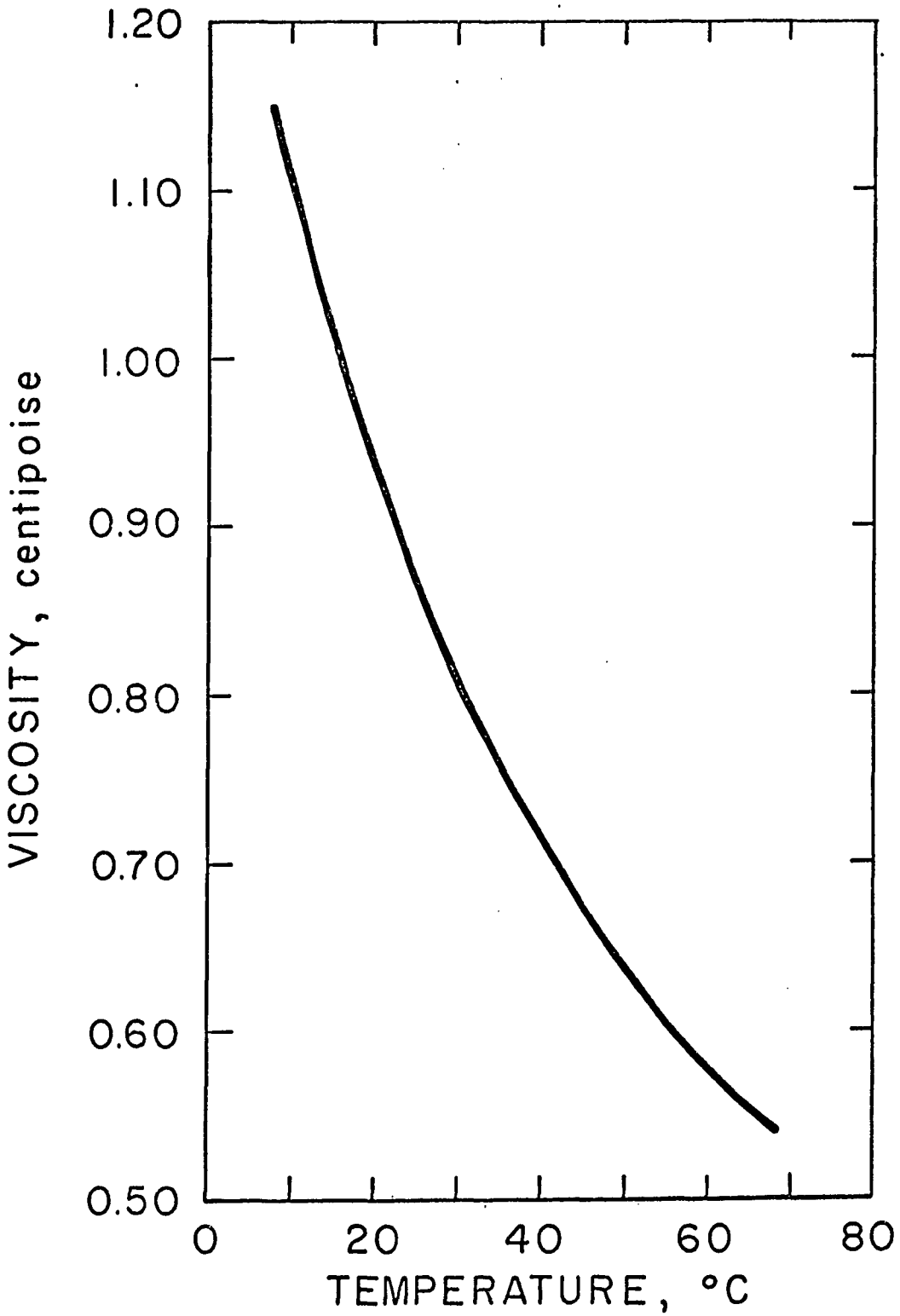

Figure C-3. Viscosity of Alpha-methylstyrene as a Function of Temperature

Reproduced with permission of the copyright owner. Further reproduction prohibited without permission.

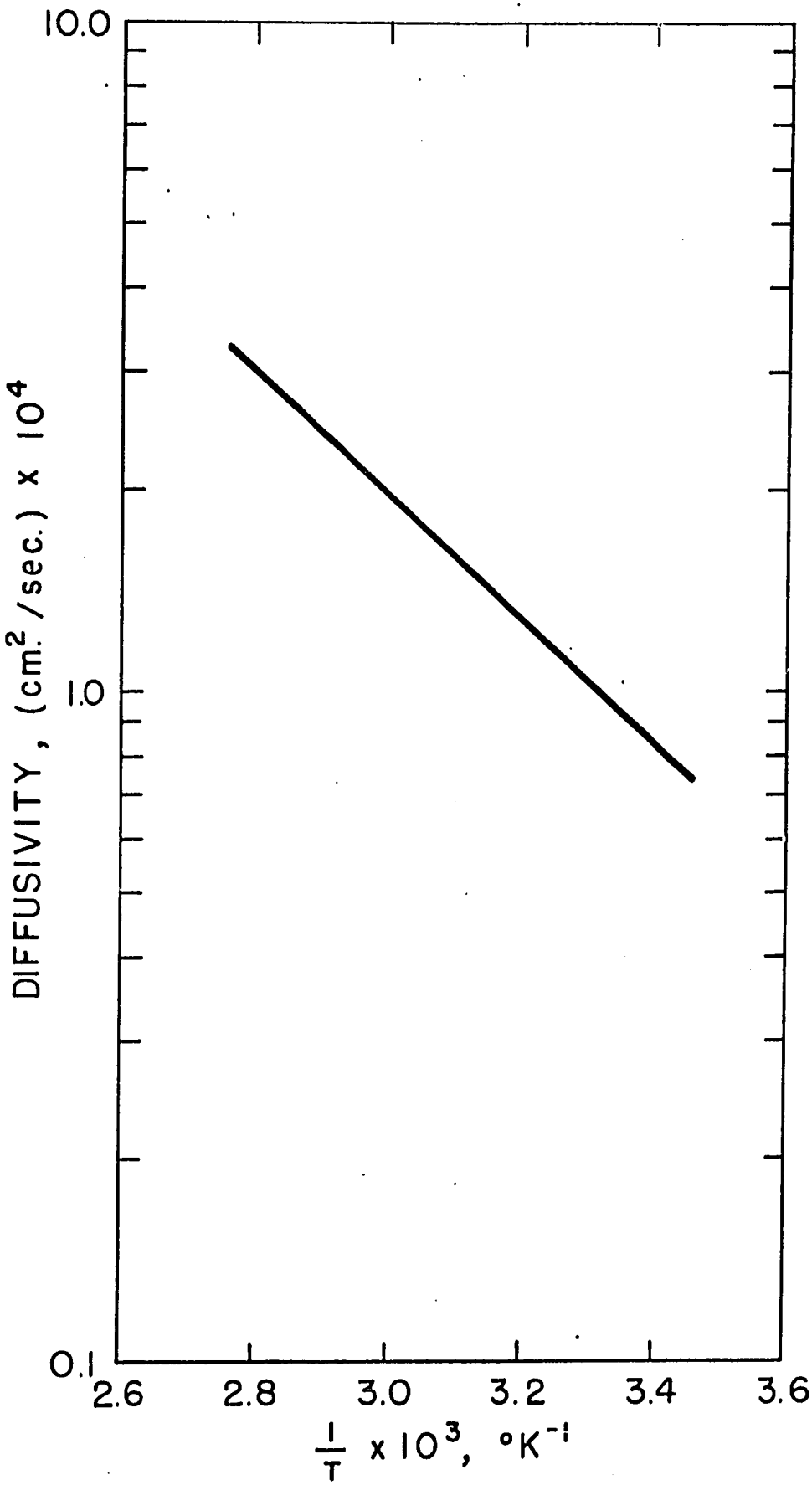

Figure C-4. Diffusivity of Hydrogen in Alpha-methylstyrene as a Function of Temperature

Reproduced with permission of the copyright owner. Further reproduction prohibited without permission.

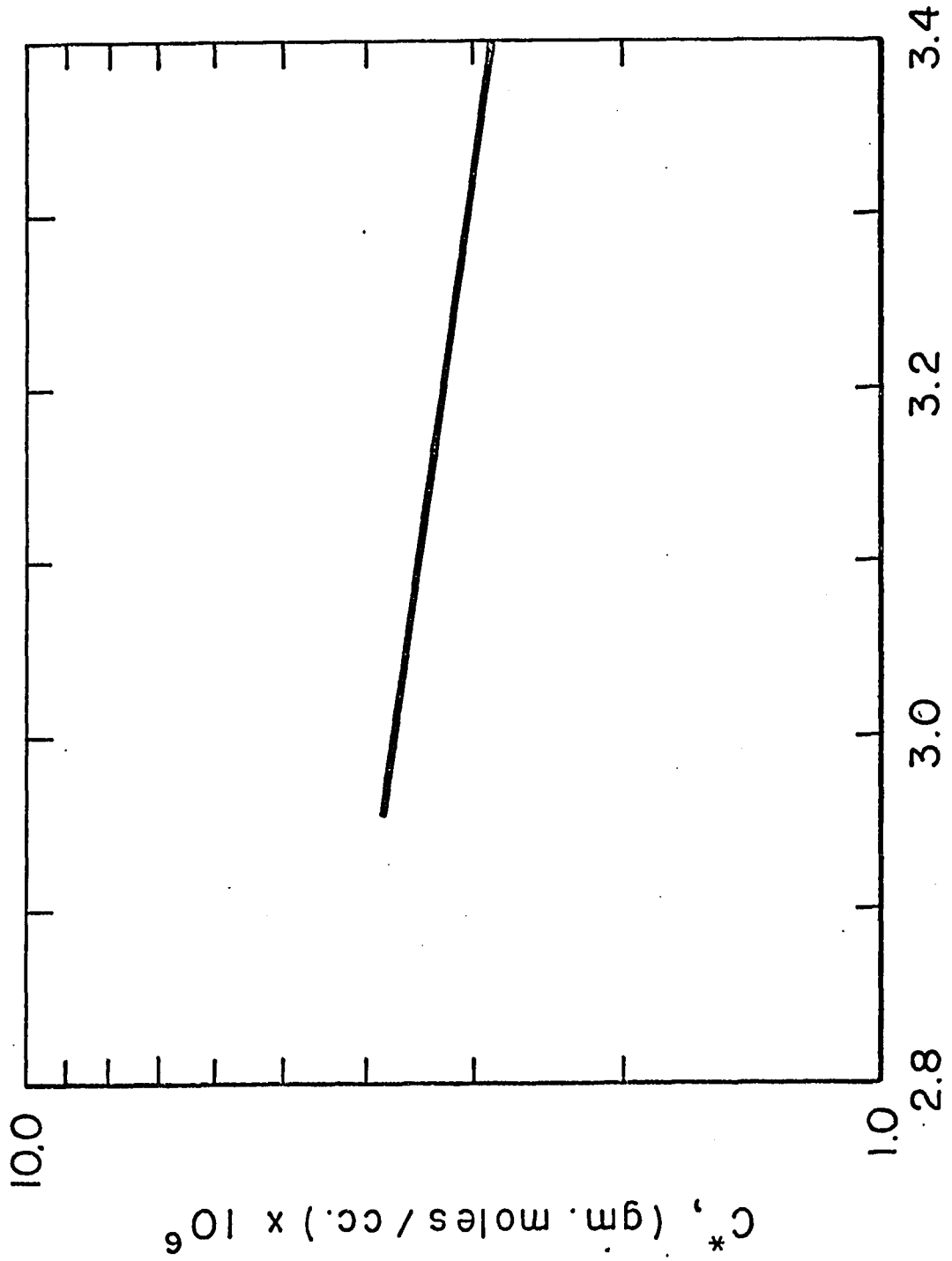

Figure C-5. Solubility of Hydrogen in Alpha-methylstyrene as a Function of Temperature at One Atmosphere Pressure

Reproduced with permission of the copyright owner. Further reproduction prohibited without permission.

NOMENCLATURE

English

A	Denotes alpha-methylstyrene molecule
AL	Denotes adsorbed alpha-methylstyrene molecule
a	Effective film area, $cm.^2/cm.^3$ bed
C	Concentration, gm. moles/cc.
C^*	Equilibrium solubility of hydrogen in alpha-methylstyrene, gm. moles/cc.
C_A, C_{H_2}, C_D	Concentration in liquid-film adjacent to solid of alpha-methylstyrene, hydrogen, and cumene, respectively
C_{AL}, C_{HL}, C_{DL}	Number of sites occupied by alpha-methylstyrene, hydrogen, and cumene, respectively
C_L	Number of vacant active sites
C_P	Number of poisoned active sites
D	Denotes cumene molecule, Equation (IV-1)
D	Diffusivity, $cm.^2/sec.$
DL	Denotes adsorbed cumene molecule
d_p	Packing granule diameter, cm.

Reproduced with permission of the copyright owner. Further reproduction prohibited without permission.

e	Logarithmic constant = 2.718
E_a	Activation energy for reaction, cal./gm. mole
F	Liquid molar flow rate, gm. moles/min.
G	Gas volumetric flow rate, liters/min.
HL	Denotes adsorbed hydrogen atom
ΔH_R	Heat of reaction, cal./gm. mole
J	Mass transfer factor, Equation (IV-5)
K_o	Overall mass transfer coefficient, Equation (IV-6), cm./sec.
k_L	Liquid-film mass transfer coefficient, cm./sec.
K_1, K_2	Adsorption equilibrium constants for alpha-methylstyrene and hydrogen, respectively
K_3	Desorption equilibrium constant for cumene
K_R	Reaction equilibrium constant
k_R, k_1, k_2, k_3	Forward reaction velocity constants
k_R', k_1', k_2', k_3'	Reverse reaction velocity constants

Reproduced with permission of the copyright owner. Further reproduction prohibited without permission.

k_o Reaction rate constant, cc. liquid/sec. - gm. catalyst

k_o' Pre-exponential factor, cc. liquid/sec. - gm. catalyst

k_s Surface reaction rate constant, Equation (IV-9)

L Liquid volumetric flow rate, cc./min.

L_T Total number of sites

MW Molecular weight, gms./gm. mole

N Molar mass flux, gm. moles/cm.^{2} sec.

N_{Re} Reynolds number, $\frac{d_p U_L \rho}{\mu}$

N_{Sc} Schmidt number, $\frac{\mu}{\rho D}$

P_{H_2} Partial pressure of hydrogen, atmospheres

r Reaction rate, gm. moles/min. - gm. catalyst

r_o Reaction rate on unpoisoned catalyst, gm. moles/min. - gm. catalyst

R Universal gas constant, cal./gm. mole ^oK

T Temperature, ^oC or ^oK

t Time, min. or sec.

U_L Average fluid velocity based on empty reactor cross section, cm./sec.

W Catalyst weight, gms.

ΔX_D Reactor conversion, gm. moles cumene/total gm. moles

Reproduced with permission of the copyright owner. Further reproduction prohibited without permission.

X_α	Mole fraction alpha-methylstyrene in an alpha-methylstyrene - cumene mixture, Equation (IV-9)
Z	Characteristic dimension through liquid film, cm.

Greek

α	Alpha, slope of deactivation curves, min^{-1}
β	Beta, constant in Equation (IV-2)
ε	Epsilon, bed void fraction, cc. voids/cc. bed
μ	Mu, viscosity, gm./cm. sec.
ρ	Rho, density, gm./cc.
σ	Sigma, standard deviation
τ	Tau, process time, min.
ϕ	Phi, deactivation function = $e^{-\alpha\tau}$

Reproduced with permission of the copyright owner. Further reproduction prohibited without permission.

LITERATURE CITED

1. Aben, P. C., J. of Catalysis, 10, 224 (1968).

2. Acres, G. J. K., Plat. Met. Rev., 11, 86 (1967).

3. Acres, G. J. K., and G. C. Bond, Plat. Met. Rev., 10 (4), 122 (1966).

4. Acres, G. J. K., and A. E. R. Budd, Brit. Pat. No. 1,089,835 (1967).

5. Amos, J. L., K. E. Coulter, and F. M. Tennant in "Styrene, Its Polymers, Copolymers and Derivatives," Chapter 15, Ed. by R. H. Boundy and R. F. Boyer (1952).

6. Babcock, B. D., G. T. Mejdell, and O. A. Hougen, A.I.Ch.E. J., 3 (3), 366 (1957).

7. Bischoff, K. B., Ind. Eng. Chem., 58 (11), 18 (1966).

8. Bischoff, K. B., A.I.Ch.E. J., 14 (5), 820 (1968).

9. Bischoff, K. B., Ind. Eng. Chem. Fundamentals, 8 (4), 665 (1969).

10. Burwell, R. L., Jr., Chem. and Eng. News, 56 (Aug. 22, 1966).

11. Calderbank, P. H., A. Caldwell, and G. Ross, Chimie et Industrie, Genie Chimique, 101, 215 (1969).

12. Carberry, J. J., and R. H. Bretton, A.I.Ch.E. J., 4 (3), 367 (1958).

13. Charpentier, J. C., C. Prost, and P. LeGoff, Chem. Eng. Sci., 24, 1777 (1969).

14. Coughlin, R. W., A.I.Ch.E. J., 15 (5), 654 (1969).

15. Craig, R. G., H. A. Forster, A. M. Henke, and S. Kwolek, The Oil and Gas Journal, May edition (1966).

Reproduced with permission of the copyright owner. Further reproduction prohibited without permission.

16. Deans, H. A., and L. Lapidus, A.I.Ch.E. J., 6 (4), 656 (1960).

17. Deans, H. A., and L. Lapidus, A.I.Ch.E. J., 6 (4), 663 (1960).

18. Dutkai, E., and E. Ruckenstein, Chem. Eng. Sci., 23, 1365 (1968).

19. Edwards, M. F., and J. F. Richardson, Chem. Eng. Sci., 23, 109 (1968).

20. Farkas, E. J., Sc.D. thesis, Massachusetts Inst. of Technology, Cambridge (1964).

21. Flory, P. J., "Principles of Polymer Chemistry," p. 132, Cornell Univ. Press, Ithaca, N.Y. (1953).

22. Freund, T., and H. M. Hulbert, J. Phys. Chem., 61, 909 (1957).

23. Glaser, M. B., and I. Lichtenstein, A.I.Ch.E. J., 9 (1), 30 (1963).

24. Glaser, M. B., and M. Litt, A.I.Ch.E. J., 9 (1), 103 (1963).

25. Gupta, A. S., and G. Thodos, A.I.Ch.E. J., 8 (5), 608 (1962).

26. Hansford, R. C., C. P. Reeg, F. C. Wood, and R. Vaell, Petro/Chem Engineer, C-6, May (1960).

27. Hochman, J. M., and E. Effron, Ind. Eng. Chem. Fundamentals, 8 (1), 63 (1969).

28. Hoftyzer, P. J., Trans. Inst. Chem. Eng., 42, T109 (1964).

29. Hofmann, H., Chem. Eng. Sci., 14, 193 (1961).

30. Hoog, H., H. G. Klinkert, and A. Schaafsma, Petroleum Refiner, 32 (5), 137 (1953).

31. Hoogendoorn, C. J., and J. Lips, Can. J. Chem. Eng., 43, 125 (1965).

Reproduced with permission of the copyright owner. Further reproduction prohibited without permission.

32. Hougen, O. A., and K. M. Watson, "Chemical Process Principles," Part 3, J. Wiley and Sons (1966).

33. Jeffreson, C. P., Chem. Eng. Sci., 23, 509 (1968).

34. Johnson, D. L., H. Saito, J. D. Polejes, and O. A. Hougen, A.I.Ch.E. J., 3 (3), 411 (1957).

35. Klassen, J., and R. S. Kirk, A.I.Ch.E. J., 1 (4), 488 (1955).

36. Kunugita, E., K. Suga, and T. Otake, J. Chem. Eng. of Japan, 2 (1), 75 (1969).

37. Lapidus, L., Ind. Eng. Chem., 49 (6), 1000 (1957).

38. Larkins, R. P., R. R. White, and D. W. Jeffrey, A.I.Ch.E. J., 7 (2), 231 (1961).

39. Levenspiel, O., and K. B.Bischoff, Adv. Chem. Eng., 4, 95 (1963).

40. Ma, Y. H., Sc.D. thesis, Massachusetts Inst. of Technology, Cambridge (1966).

41. Maxted, E. B., Adv. in Cat., 3, 129 (1951).

42. Molstad, M. C., J. F. McKinney, and R. G. Abbey, Trans. Am. Inst. Chem. Eng., 39, 605 (1943).

43. Murphree, E. V., A. Voorhies, and F. X. Mayer, Ind. Eng. Chem. Proc. Des. Dev., 3 (4), 381 (1964).

44. Olbrich, W. E., and J. D. Wild, Chem. Eng. Sci., 24, 25 (1969).

45. Onda, K., E. Sada, C. Kido, and A. Tanaka, Kagaku Kogaku, 1 (1), 50 (1963).

46. Onda, K., E. Sada, and Y. Murase, A.I.Ch.E. J., 5 (2), 235 (1959).

47. Pelossof, A. A., Sc.D. thesis, Massachusetts Inst. of Technology, Cambridge (1967).

48. Raines, G. E., and T. E. Corrigan, Chem. Eng. Progr. Symp. Series No. 72, 63, 90 (1967).

Reproduced with permission of the copyright owner. Further reproduction prohibited without permission.

49. Reiss, L. P., Ind. Eng. Chem. Proc. Des. Dev., 6 (4), 486 (1967).

50. Ross, L. D., Chem. Eng. Progr., 61 (10), 77 (1965).

51. Sater, V. E., and O. Levenspiel, Ind. Eng. Chem. Fundamentals, 5 (1), 86 (1966).

52. Satterfield, C. N., A. A. Pelossof, and T. K. Sherwood, A.I.Ch.E. J., 15 (2), 226 (1969).

53. Sawyer, D. N., and R. Mezaki, A.I.Ch.E. J., 13 (6) 1221 (1967).

54. Schiesser, W. E., and L. Lapidus, A.I.Ch.E. J., 7 (1), 163 (1961).

55. Sherwood, T. K., and E. J. Farkas, Chem. Eng. Sci., 21, 573 (1966).

56. Sherwood, T. K., and F. A. L. Holloway, Trans. Amer. Inst. Chem. Engrs., 36, 21 (1940).

57. Sherwood, T. K., and F. A. L. Holloway, Trans. Amer. Inst. Chem. Engrs., 36, 39 (1940).

58. Shulman, H. L., C. F. Ullrich, A. Z. Proulx, and J. O. Zimmerman, A.I.Ch.E. J., 1 (2), 253 (1955).

59. Smith, H. A., in Catalysis, Vol V, Ch. 4 (1957).

60. Sokol'skii, D. V., "Hydrogenation in Solutions," Pub. in USA by D. Davey and Co., N.Y. (1964).

61. Sweeney, D. E., A.I.Ch.E. J., 13 (4), 663 (1967).

62. Szépe, S., and O. Levenspiel, paper presented at Fourth European Symposium on Chemical Reaction Engineering, Brussels, Sept. 1968.

63. Taha, H., Ph.D. thesis, University of Maryland, College Park (1969).

64. Turpin, J. L., and R. L. Huntington, A.I.Ch.E. J., 13 (6), 1196 (1967).

Reproduced with permission of the copyright owner. Further reproduction prohibited without permission.

65. Unzelman, G. H., and N. H. Gerber, Petro/Chem Engineer, 32, October (1965).

66. van Deemter, J. J. Chemical Reaction Engineering, Proceedings of the Third European Symposium, held in Amsterdam, 15-17 September (1964).

67. van den Bleek, C. M., K. van der Wiele, and P. J. van den Berg, Chem. Eng. Sci., 24, 681 (1969).

68. van Krevelen, D. W., and J. T. C. Krekels, Rec. Trav. Chem., 67, 512 (1948).

69. van Swaaij, W. P. M., J. C. Charpentier, and J. Villermaux, Chem. Eng. Sci., 24, 1083 (1969).

70. Watt, G. W., and M. T. Walling, Jr., J. Phys. Chem., 59, 7 (1955).

71. Weekman, V. W., Jr., Ind. Eng. Chem. Proc. Des. Dev., 7 (1), 90 (1968).

72. Weekman, V. W., Jr., and J. E. Myers, A.I.Ch.E. J., 10 (6), 951 (1964).

73. Wen, C. Y., W. S. O'Brien, and L. T. Fan, J. Chem. and Eng. Data, 8 (1), 42 (1963).

74. Wen, C. Y., W. S. O'Brien, and L. T. Fan, J. Chem. and Eng. Data, 8 (1), 47 (1963).

75. Wheeler, A., Adv. in Cat., 3 (1951).

76. Williamson, J. E., K. E. Bazaire, and C. J. Geankoplis, Ind. Eng. Chem. Fundamentals, 2 (2), 126 (1963).

77. Wilson, E. J., and C. J. Geankoplis, Ind. Eng. Chem. Fundamentals, 5 (1), 9 (1966).

Reproduced with permission of the copyright owner. Further reproduction prohibited without permission.

VITA

Name: Albert Russell Hoge.

Permanent address: 4417 Romlon Street,
Beltsville, Maryland 20705.

Degree and date to be conferred: Ph.D., 1970.

Date of birth: August 25, 1943.

Place of birth: Darby, Pennsylvania.

Secondary education: Swarthmore High School, 1961.

Collegiate institutions attended:

	Dates	Degree	Date of Degree
University of Delaware	1961-65	B.Ch.E.	1966
University of Maryland	1965-70	Ph.D.	1970

Major: Chemical Engineering.

Minor(s): Chemistry, Nuclear Engineering.

Publications: "Thermal Conductivity of Polymers," with T. G. Smith, Society of Plastics Engineers' Journal, 23 (4), 67 (1967).

Positions held: Engineer,
Scott Paper Company,
Philadelphia, Pennsylvania.

Teaching Assistant,
University of Maryland,
College Park, Maryland.

NDEA Fellow
University of Maryland,
College Park, Maryland.

Prospective position: Process Research Engineer,
Hydrocarbons and Polymers Division,
Monsanto Company,
Springfield, Massachusetts.

Reproduced with permission of the copyright owner. Further reproduction prohibited without permission.